DOI: 10.26599/FSHW.2025.9250829

Contents lists available at SciOpen

Food Science and Human Wellness

journal homepage: https://www.sciopen.com/journal/2097-0765

China Food Publishing Co.

Coenzyme Q10 Alleviates Renal Injury through Modulating Lipid Metabolism in ApoE-deficient Mice Fed a High-fat Diet Based on Lipidomic Analysis

Junyu Ma[1#], Chunting Wu[1#], Rong Li[1#], Mengyao Li[1], Xiaoyan Bi[1], Bangzhao Zeng[1], Xuexun Li[1], Xin Zhao[1], Chunmei Zhang[2*], Fuli Ya[1*]

[1]*Department of Nutrition, School of Public Health, Dali University, Dali, Yunnan 671000, China*

[2]*Department of Laboratory Teaching Center, School of Public Health, Dali University, Dali, Yunnan 671000, China*

ABSTRACT: Dyslipidemia is a significant risk factor for chronic kidney disease (CKD). Coenzyme Q10 (CoQ10), commonly recognized as a dietary supplement, exhibits a wide range of biological activities. This study aimed to investigate the efficacy of CoQ10 in mitigating renal damage in apolipoprotein E-deficient ($ApoE^{-/-}$) mice subjected to a high-fat diet (HFD). The findings revealed that a 12-week supplementation of CoQ10 (1800 mg/kg diet) significantly decreased HFD-induced elevations in levels of renal function parameters, including serum uric acid (SUA; from (54.84 ± 6.35) to (37.96 ± 5.25) μmol/L; $P < 0.001$), creatinine (SCr; from (22.72 ± 2.69) to (14.02 ± 2.72) μmol/L; $P < 0.001$), and blood urea nitrogen (BUN; from (5.79 ± 0.65) to (3.70 ± 1.01) mmol/L; $P < 0.001$). Moreover, CoQ10 supplementation significantly ameliorated HFD-induced pathological alterations, lipid accumulation ($P < 0.01$), oxidative stress ($P < 0.01$), inflammation ($P < 0.05$), and fibrosis ($P < 0.01$) in the kidneys. Furthermore, untargeted lipidomics analysis of the kidneys demonstrated that CoQ10 effectively promoted the recovery of differential lipid species, primarily including glycerophospholipids (GP), glycerolipids (GL), and sphingolipids (SP) in HFD-fed mice ($P < 0.05$). Additionally, targeted lipidomic analysis of GP suggested that a HFD led to an increase in renal concentrations of various lipid metabolites, primarily within the osphatidylcholines (PC) and 1-(1Z-alkenyl),2-acylglycerophosphoethanolamines (PE_P) classes. These alterations were favorably restored by CoQ10 supplementation ($P < 0.05$). Furthermore, Western blot analysis demonstrated that CoQ10 significantly downregulated renal PI3K/Akt ($P < 0.01$) and TLR4/MyD88/NFκB ($P < 0.05$) signaling pathways in HFD-fed mice. Consequently, this study suggests that CoQ10 exerts a potent regulatory effect on lipid metabolism disorders induced by a HFD, thereby contributing to the mitigation of renal injury under hyperlipidemic conditions.

Keywords: Coenzyme Q10, chronic kidney disease, renal injury, lipid metabolism, high-fat diet, apolipoprotein E-deficient mice

1. Introduction

The incidence and prevalence of chronic kidney disease (CKD) are increasing globally. CKD is a major contributor to morbidity and mortality worldwide, affecting over 10% of the global population, which translates to more than 800 million individuals[1]. Numerous risk factors have been identified that may induce or exacerbate CKD, with hyperlipidemia, diabetes mellitus, and obesity being recognized as primary

[#]Junyu Ma, Chunting Wu and Rong Li contributed equally to this work.
***Corresponding author**
yafuli@yeah.net; ZhangCM2023@yeah.net

Received 22 April 2025
Received in revised from 17 June 2025
Accepted 25 July 2025

contributors[2]. A disruption in lipid metabolism is a common characteristic feature of these risk factors, influencing the stages, progression, and prognosis of CKD[3]. Dyslipidemia is also a hallmark of CKD and is believed to contribute to the onset of cardiovascular diseases (CVDs), which are the leading cause of death among patients with mild to moderate CKD and those with end-stage renal disease[4]. Improving lipid profiles has been shown to be an effective strategy in decelerating the progression of CKD[5]. Several novel lipid-targeting agents have been developed, and some are currently undergoing clinical trials in the context of CKD, fostering optimism for further therapeutic advancements in this area[6].

Dietary lipids, particularly triglycerides, constitute over 30% of the total energy intake in Western diets. Prolonged consumption of a high-fat diet (HFD) induces significant modifications in renal lipid metabolism and lipotoxicity, culminating in renal injury. Alterations in cholesterol and fatty acid metabolism, for instance, contribute to damage in glomerular and tubular cells[6]. Fatty acids are fundamental to the synthesis of complex lipids. The kidney, an organ with high energy demands, predominantly relies on fatty acid oxidation (FAO) for energy[7]. In CKD, disruptions in FAO, lipid uptake, and lipogenesis lead to intracellular lipid accumulation, ultimately resulting in functional loss and fibrosis. Impaired and inefficient FAO in the proximal tubule is considered a primary mechanism of kidney injury and subsequent fibrosis[8]. Lipid droplet accumulation is a characteristic feature of CKD; intracellular lipid deposition induces oxidative stress and inflammation, which are critical in the initiation and progression of kidney fibrosis[6]. The mechanisms underlying the accumulation of renal lipids remain poorly understood and may vary across CKD of different etiologies. Furthermore, substantial changes in renal lipid compositions and aberrant lipid metabolism induced by a HFD are closely linked to renal injury and the progression of CKD[4]. While dyslipidemia associated with CKD has been extensively investigated, the role of renal lipid dysmetabolism in the progression of CKD remains less well understood[3, 6].

Dietary composition interventions represent a critical strategy for the prevention and/or deceleration of CKD progression[9, 10]. Recent research underscores the significant protective influence of specific dietary patterns in modulating CKD progression, such as the Mediterranean diet, Dietary Approaches to Stop Hypertension (DASH), and vegetarian diets[11, 12]. Coenzyme Q10 (CoQ10), a lipophilic molecule present in a diverse array of foods, is ubiquitously expressed in eukaryotic cells where it functions as a mitochondrial electron carrier and co-factor for mitochondrial enzymes[13]. CoQ10 is widely recognized as a dietary supplement that supports various health functions, including cardiovascular protection[13]. Our previous studies have demonstrated that CoQ10 supplementation can improve lipid profiles, decreased platelet hyperreactivity, and consequently offer protection against CVDs in dyslipidemic patients[14] and in apolipoprotein E-deficient ($ApoE^{-/-}$) mice subjected to a HFD[15]. Furthermore, several studies have suggested that CoQ10 supplementation exerts significant preventive effects in CKD[16]. Nonetheless, the effect of CoQ10 on renal lipid metabolism and kidney injury under hyperlipidemic conditions remains inadequately understood. This study aimed to investigate the protective effects of CoQ10 supplementation against renal injury and its underlying mechanisms in an atherosclerosis model using HFD-fed $ApoE^{-/-}$ mice.

2. Material and methods

2.1 Chemicals and reagents

CoQ10 was purchased from Sigma-Aldrich (St. Louis, MO, USA). Antibodies against PI3K (CAT#AF6241), phospho-PI3K (Tyr^{607}) (CAT#AF3241), Akt (CAT#AF6261), phospho-Akt (Ser^{473}) (CAT#AF0016), TLR4 (CAT#AF7017), MyD88 (CAT#AF5195), TNF-α (CAT#AF7014), IL-1β (CAT#AF5103), phospho-AMPK (Thr^{172}) (CAT#AF3423) and β-tubulin (CAT#AF7011) were purchased from Affinity Biosciences (OH, USA). Antibodies against NFκB p65 (CAT#BS1257), phospho-NFκB p65 (Ser^{536}) (CAT#BS4138), IκBα (CAT#BS3601), phospho-IκBα (Tyr^{42}) (CAT#BS4736), AMPK (CAT#BS1009), ACD (CAT#BS60618), CPT1A (CAT#BS7744), GAPDH (CAT#AP0063) and β-actin (CAT#AP0060) were purchased from Bioworld Technology (MN, USA). Antibody against IL-6 (CAT#GB11117) and secondary antibodies including horseradish peroxidase (HRP)-conjugated goat anti-rabbit IgG (CAT#GB23303) and anti-mouse IgG (CAT#GB23301) were purchased from Servicebio (Wuhan, China). Antibody against PPARα (CAT#TA503545S) was purchased from OriGene (MD, USA).

2.2 Animals and diets

Eight-week-old male homozygous $ApoE^{-/-}$ mice, with a C57BL/6 background, were procured from The Jackson Laboratory. The mice were maintained in a specific-pathogen-free (SPF) facility, and housed under standard conditions, which included a 12-hour light-dark cycle at a temperature of 22-24℃. The animals had unrestricted access to food and water. Following a two-week acclimatization period, the mice were randomly allocated into four experimental groups. These groups were fed for 12 weeks with either a standard AIN-93G diet (ND group), an AIN-93G diet supplemented with CoQ10 at a concentration of 1800 mg/kg diet (ND+CoQ10 group), a high-fat diet (HFD) containing 21% fat (HFD group), or a HFD supplemented with CoQ10 at the same concentration (HFD+CoQ10 group). Throughout the feeding period, body weight and food intake were recorded weekly. CoQ10 powder was thoroughly mixed into the respective diets. The animal feeds were sourced from Medicience Ltd. (Jiangsu, China), with their compositions detailed in **Supplementary Table S1**. The CoQ10 dosage was based on our prior studies[15, 17, 18]. All experimental procedures were approved by the Animal Care and Use Committee of Dali University (Permit number: SYXK [Dian] 2018-0002).

2.3 Blood and kidney tissue collection

Following a 12-week intervention period, mice were anesthetized after an eight-hour fasting period using an intraperitoneal injection of 10% chloral hydrate (0.02 mL/g body weight). Blood samples were obtained via cardiac puncture and collected into tubes containing 1/10 volume of 3.8% acid citrate dextrose (38 mmol/L citric acid, 75 mmol/L trisodium citrate, 100 mmol/L dextrose) as an anticoagulant. Subsequently, the anticoagulated blood was centrifuged at 2500 × *g* for 15 min at 4℃. The resulting supernatant was transferred to a new tube and stored at -80 ℃ for future analysis. Following blood collection, the vasculature was perfused

with saline through the left ventricle to remove blood from the mice after the thoracic cavity was opened. Kidney tissue was then harvested and weighted.

2.4 Hematoxylin-eosin (HE) staining

HE staining was performed as previously described[10, 19, 20]. Briefly, freshly harvested kidneys were bisected, fixed in 4% paraformaldehyde (PFA, pH 7.2), and embedded in paraffin. Kidney sections, 5 μm in thickness, were stained with HE for morphological assessment. The sections were digitized using a Leica microscope (Leica Microsystems, Heidelberg, Germany).

2.5 Masson staining

Masson staining was employed to detect fibrosis in kidney tissue samples. Briefly, following deparaffinization, the kidney tissue sections were treated with Weigert's hematoxylin for 10 min, followed by staining with Masson blue and ponceau magenta for 5 min. Subsequently, the sections were rinsed with a phosphomolybdic acid solution and then immersed in aniline blue for 2 min. The sections were then dehydrated, cleared with xylene, and mounted. The nuclei and collagen fibers were visualized as blue, while the cytoplasm, muscle fibers, and erythrocytes appeared red. The collagen volume fraction was calculated using the formula: collagen volume fraction (%) = (collagen-positive area (blue)/total area of image) × 100%.

2.6 Determination of serum creatinine (SCr), serum uric acid (UA), blood urea nitrogen (BUN) and renal lipid contents

The levels of SCr, UA and BUN were quantified using an automatic biochemical analyzer (Beckman Instruments, Inc., California, USA). Levels of total cholesterol (TC) and triglycerides (TG) in the kidney were measured using commercial assay kits from Nanjing Jiancheng Bio Co. (Nanjing, China), following the manufacturer's instructions. Free fatty acid (FFA) levels in the kidney were assessed using a commercial assay kit provided by Sangon Biotech Co., Ltd. (Shanghai, China).

2.7 Measurement of total antioxidant capacity (T-AOC), superoxide dismutase (SOD) activity, and malonaldehyde (MDA)

The levels of T-AOC, SOD activity, and MDA in kidney tissue were measured using a T-AOC Assay Kit, SOD Activity Assay Kit (Beijing Boxbio Science & Technology Co., Ltd., Beijing, China), and MDA Assay Kit (Nanjing Jiancheng Co., Nanjing, China), respectively. Briefly, tissue homogenization (100 mg) was conducted in an ice bath for 15 min, followed by centrifugation at 10000 × *g* for 10 min at 4℃ to eliminate insoluble materials. The resulting supernatant was transferred to a new tube, maintained on ice, and the protein concentrations were subsequently assessed. The T-AOC, SOD activity, and MDA levels were then determined in accordance with the manufacturer's instructions. Absorbance measurements were taken using a microplate reader at wavelengths of 560 nm for SOD activity, 593 nm for T-AOC, and 532 nm for MDA. The SOD activity, T-AOC, and MDA levels were calculated and expressed as units/mg protein, μmol/mg protein and nmol/g tissue weight, respectively.

2.8 Western blotting analysis

Kidney tissues were homogenized in RIPA lysis buffer containing protease/phosphatase inhibitors (Beyotime Biotechnology Corporation, Shanghai, China) using a tissue homogenizer (Servicebio Technology Co., Ltd., Wuhan, China). Lysates were centrifuged at 12000 × *g* for 15 min at 4℃, and supernatants were collected for protein quantification using a BCA protein assay kit (KeyGEN Biotechnology, Nanjing, China). Total protein (30 μg) was denatured, separated by sodium dodecyl sulfate-polyacrylamide gel electrophoresis (SDS-PAGE), and electrotransferred to polyvinylidene difluoride (PVDF) membranes (Millipore, MA, USA). Immunoblotting was performed according to our previously described methods[21, 22]. Briefly, following blocking with 5% BSA for 1.5 h, the PVDF membrane was incubated overnight at 4℃ with primary antibodies against the following targets (dilutions in parentheses): PI3K (1:2000), phospho-PI3K (Tyr^{607}) (1:2000), Akt (1:2000), phospho-Akt (Ser^{473}) (1:2000), TLR4 (1:2000), MyD88 (1:2000), phospho-NFκB p65 (Ser^{536}) (1:1000), NFκB p65 (1:1000), phospho-IκB (Tyr^{42}) (1:1000), IκB (1:2000), TNF-α (1:500), IL-1β (1:2000), IL-6 (1:1000), PPARα (1:500), AMPK (1:1000), phospho-AMPK (Thr^{172}) (1:2000), SCD (1:1000), CPT1A (1:1000), GAPDH (1:10000), β-tubulin (1:5000) and β-actin (1:10000) at 4℃ overnight and then washed 3 times in TBST. Subsequently, the membrane was washed three times with TBST and then incubated for 1.5 h with HRP-conjugated goat anti-rabbit IgG (1:20000) and goat anti-mouse IgG (1:10000) secondary antibodies. After three additional TBST washes, protein bands were visualized using an ECL Western blotting detection system. GAPDH, β-tubulin and β-actin served as loading controls. Protein band intensities were quantified using ImageJ software (version 1.37v; NIH, USA) and normalized to the corresponding loading control.

2.9 Statistical analysis

Data were collected from at least three independent mice and represented as means with standard deviation (mean ± SD). One-way analysis of variance (ANOVA) followed by Tukey's multiple comparisons test was conducted to determine the statistical significance using GraphPad Prism software (version 9.4.1; GraphPad Inc., San Diego, CA, USA). Spearman's rank correlation analysis assessed relationships between differential lipids and biological parameters. Differences between groups were considered statistically significant at *P*-value below 0.05.

2.10 Lipidomics analysis

2.10.1 Untargeted lipidomics analysis by UPLC-TOF/MS

For untargeted lipidomics analysis, kidney tissue samples (50 mg wet weight) were homogenized in 200 μL of ice-cold 50% methanol (v/v) using a Precellys 24 homogenizer (JXFSTPRP-CLN, Shanghai, China) with two 3.0 mm stainless steel grinding beads at 6000 r/min for 30 s (2 cycles, 4℃). To the homogenate, 600 μL of ice-cold methyl tert-butyl ether (MTBE) was added, followed by vortex mixing for 30 min at 4℃. After phase separation by centrifugation at 3000 r/min for 15 min at 4℃, 200 μL of the upper organic phase was transferred to a fresh 1.5 mL microcentrifuge tube. The extract was lyophilized in a FreeZone 2.5 L freeze-dryer (Labconco CentriVap, USA) and reconstituted in 200 μL of dichloromethane:methanol (1:1, v/v) with 0.01% butylated hydroxytoluene (BHT). After centrifugation

(3000 × *g*, 15 min, 4℃), the supernatant was transfered to a vial for UPLC-HRMS (Ultra Performance Liquid Chromatography-High Resolution Mass Spectrometry) detection. Quality control (QC) samples were prepared by pooling equal aliquots of all reconstituted extracts.

Chromatographic separation was performed on an ACQUITY UPLC CSH C18 column (100 mm × 2.1 mm, 1.7 μm; Waters) maintained at 40℃ using a binary gradient at 0.3 mL/min. The mobile phase consisted of phase A (10 mmol/L ammonium formate + 0.1% formic acid in acetonitrile:water (60:40, v/v)) and phase B (10 mmol/L ammonium formate + 0.1% formic acid in isopropanol:acetonitrile (90:10, v/v)). Gradient elution conditions were set as follows: (0–0.4) min: 30% B; (0.4–1.0) min: 30%→45% B; (1.0–3.5) min: 45%→60% B; (3.5–5.0) min: 60%→75% B; (5.0–7.0) min: 75%→90% B; (7.0–8.5) min: 90%→100% B; (8.5–8.6) min: 100% B (hold); (8.6–8.61) min: 100%→30% B; (8.61-10.0) min: 30% B (equilibration). The injection volume for each sample was 4 μL. Mass spectrometry was performed on a high-resolution tandem mass spectrometer TripleTOF^{TM} 6600 system (SCIEX, NL) equipped with DuoSpray™ ion source. Data acquisition in both positive (+5000 V) and negative (-4500 V) electrospray ionization (ESI) modes used the following parameters: source temperature: 500℃; curtain gas: 30 psi; nebulizer gas (Gas 1) and heater gas (Gas 2): 60 psi; declustering potential: 80 V. Full-scan MS (m/z 50-2000) with 170 ms accumulation time was followed by information dependent acquisition IDA of the top 12 most intense ions exceeding 100 cps. MS/MS scans (m/z 25-1200) used 30 ms accumulation time, collision energy spread of (35 ± 15) eV, and dynamic exclusion for 8 s after 2 occurrences.

2.10.2 Targeted lipidomics analysis of glycerophospholipids by UPLC-MS/MS

For targeted lipidomics analysis, kidney tissue samples (10 mg wet weight) were transferred to Precellys® lysing tubes containing 1.4 mm ceramic beads. After adding 20 μL ice-cold ultrapure water, homogenization was performed using a BB24 Bullet Blender (Next Advance, Inc., NY, USA) at 6 m/s for 3 min at 4℃. Subsequently, 300 μL of ice-cold methanol containing the deuterated internal standards was added. The information of internal standards was depicted in **Supplementary Table S2**. Samples were re-homogenized (6 m/s, 3 min, 4℃), then centrifuged at 18000 × g for 20 min at 4℃. A 150 μL aliquot of supernatant was transferred to a polypropylene 96-well plate.

Chromatographic separation was performed on an ACQUITY® UPLC I-Class/Xevo® TQ-S System. A BEH C18 (100 mm × 2.1mm, 1.7 μm, Waters) was used for separation and maintained at 40℃ using a Vanquish UPLC system (Thermo Scientific). Mobile phase consisted of phase A (5 mmol/L ammonium acetate in HPLC-grade water) and phase B (5 mmol/L ammonium acetate in methanol). Gradient program at 0.3 mL/min: (0–1.0) min: 60% B→80% B; (1.0–4.0) min: 80% B→95% B; (4.0–7.0) min: 95% B (hold); (7.0–7.1) min: 95% B→60% B; (7.1–9.0) min: 60% B (equilibration); injection volume: 5 μL (maintained at 10℃ in autosampler). Detection utilized a Xevo® TQ-S triple quadrupole mass spectrometer (Waters) with positive ESI mode under these parameters: capillary voltage: +3.0 kV; source temperature: 550℃; desolvation gas (N_2): 800 L/h; cone gas (N_2): 150 L/h; nebulizer gas: 7.0 bar; collision gas (Ar): 0.15 mL/min. Multiple

reaction monitoring (MRM) transitions were optimized for glycerophospholipid species with individual dwell times (10–50 ms). Collision energies ranged from 20–45 eV depending on lipid class.

2.10.3 Quality control for lipidomic analysis

For untargeted lipidomics, QC pools (n=6) were injected every six samples to ensure system stability. QC involved monitoring total ion chromatogram (TIC) stability monitoring, selecting high-quality features (using K-nearest neighbors (KNN) imputation, probabilistic quotient normalization (PQN) normalization, and coefficient of variation (CV) filtering), conducting multivariate analyses (principal component analysis (PCA) and hierarchical clustering), and assessing correlations. All batches met validation criteria: QC feature CV < 30%, inter-QC correlation r > 0.95, and PCA dispersion < 2% total variance. QC TICs showed over 90% visual overlap **(Supplementary Fig. S1A-1B)**. Features with > 50% missingness in QCs or > 80% in study samples were excluded. KNN imputation (k = 10) and PQN with median QC as reference were used. Features with CV > 30% in QCs were discarded. Boxplots indicated consistent overall peak intensities **(Supplementary Fig. S1C)**. QC samples were tightly clustered on the heat map with similar metabolite intensities, indicating minimal differences and high consistency **(Supplementary Fig. S1D)**. Pairwise Pearson correlation of log-transformed intensities showed QC-QC correlations of r ≥0.95 **(Supplementary Fig. S1E)**. CV distribution revealed 80% of metabolites had CV < 25% in biological replicates, with the QC CV curve in the top-left quadrant **(Supplementary Fig. S1F)**. PCA confirmed all QCs were within the 95% confidence ellipse, with an average QC PC1/PC2 shift of < 2% of total variance. These results indicate effective quality control.

For targeted analysis, pooled biological quality control (PBQC) samples, composed of nine kidney samples, were included with each batch. PBQC samples were strategically placed at the beginning and end of each sample set to assess system stability. The acceptance criteria were defined as follows: a retention time shift of less than 0.1 minutes, an internal standard relative standard deviation (ISTD RSD) of less than 15%, and a mass error of less than 5 parts per million (ppm). Inter-batch normalization was conducted using PBQC-based correction when the CV for the batch exceeded 15%.

2.10.4 Lipidomic data processing and analysis

MS data pretreatment, including peak picking, grouping, retention time correction, and isotope/adduct annotation, was conducted using XCMS software. LC-MS raw data were converted to mzML format and processed with XCMS and the MetaboAnnotation toolbox in R software (version 4.1.1). Ions were identified by retention time and *m/z* data, and peak intensities were recorded to create a 3D matrix of peak indices, sample names, and ion intensities. Metabolites were annotated using the KEGG and HMDB databases by matching sample *m/z* data. Peak intensity data underwent further preprocessing in R software. Group comparisons used one-way ANOVA with Tukey's *post hoc* testing ($\alpha = 0.05$). *P*-values underwent false discovery rate (FDR) correction via Benjamini-Hochberg method. Discriminatory features were identified through supervised partial least squares-discriminant analysis (PLS-DA) in R. Biological relevance was assigned to features with variable importance in projection (VIP) scores > 1.0.

3. Results

3.1 CoQ10 alleviated renal injury in HFD-fed mice

To determine the efficacy of CoQ10 supplementation in mitigating renal injury induced by hyperlipidemia, ApoE$^{-/-}$ mice were fed on a standard AIN-93G diet or a HFD, with or without CoQ10 supplementation (0.18% of the diet) for a duration of 12 weeks, as depicted in **Fig. 1A**. Our findings revealed that the plasma concentration of CoQ10 reached (3.196 ± 0.511) μmol/L, representing a 20.3-fold increase compared to the HFD-fed mice[15]. This result indicates that CoQ10 is effectively absorbed systemically following 12 weeks of supplementation. As shown in **Fig. 1B**, the body weight of mice in the HFD group was significantly higher than that of the ND group from the 8th week to the 12th week; CoQ10 supplementation did not significantly affect body weight **(Fig. 1B)**. Moreover, no significant differences in food intake were observed among the four groups throughout the experimental period **(Fig. 1C)**. Furthermore, renal weight in the HFD group was greater than that in the ND group at the conclusion of the 12th week, but was decreased in the HFD+CoQ10 group due to CoQ10 supplementation **(Fig. 1D)**. Although the renal coefficient did not differ significantly between the HFD and ND groups, there was a trend indicating an increased effect in the HFD group, which was notably decreased by CoQ10 supplementation **(Fig. 1E)**. Additionally, our previous research demonstrated that CoQ10 supplementation favorably improved the plasma lipid profile in HFD-fed mice within this animal model, including reductions in plasma levels of TC, TG and low-density lipoprotein cholesterol (LDL-C)[15].

We further determined the effect of CoQ10 supplementation on renal injury in mice. Compared to the ND group, the HFD group exhibited elevated levels of renal function parameters, including SCr, UA and BUN; these parameters were significantly improved by CoQ10 supplementation **(Fig. 1F-1H)**. Moreover, HE staining of kidney sections revealed normal histology in both the ND and ND+CoQ10 groups. In contrast, kidney tissue from the HFD group displayed significant pathological alterations, such as irregular contours and structural disintegration in the glomerular Bowman's capsule. Additionally, renal tubular epithelial cells in HFD-fed mice exhibited vacuolar degeneration, with severe brush border disruption and epithelial sloughing **(Fig. 1I)**. These pathological alterations were effectively ameliorated by CoQ10 supplementation **(Fig. 1I)**. Collectively, these findings demonstrate that CoQ10 alleviates HFD-induced renal injury in ApoE$^{-/-}$ mice.

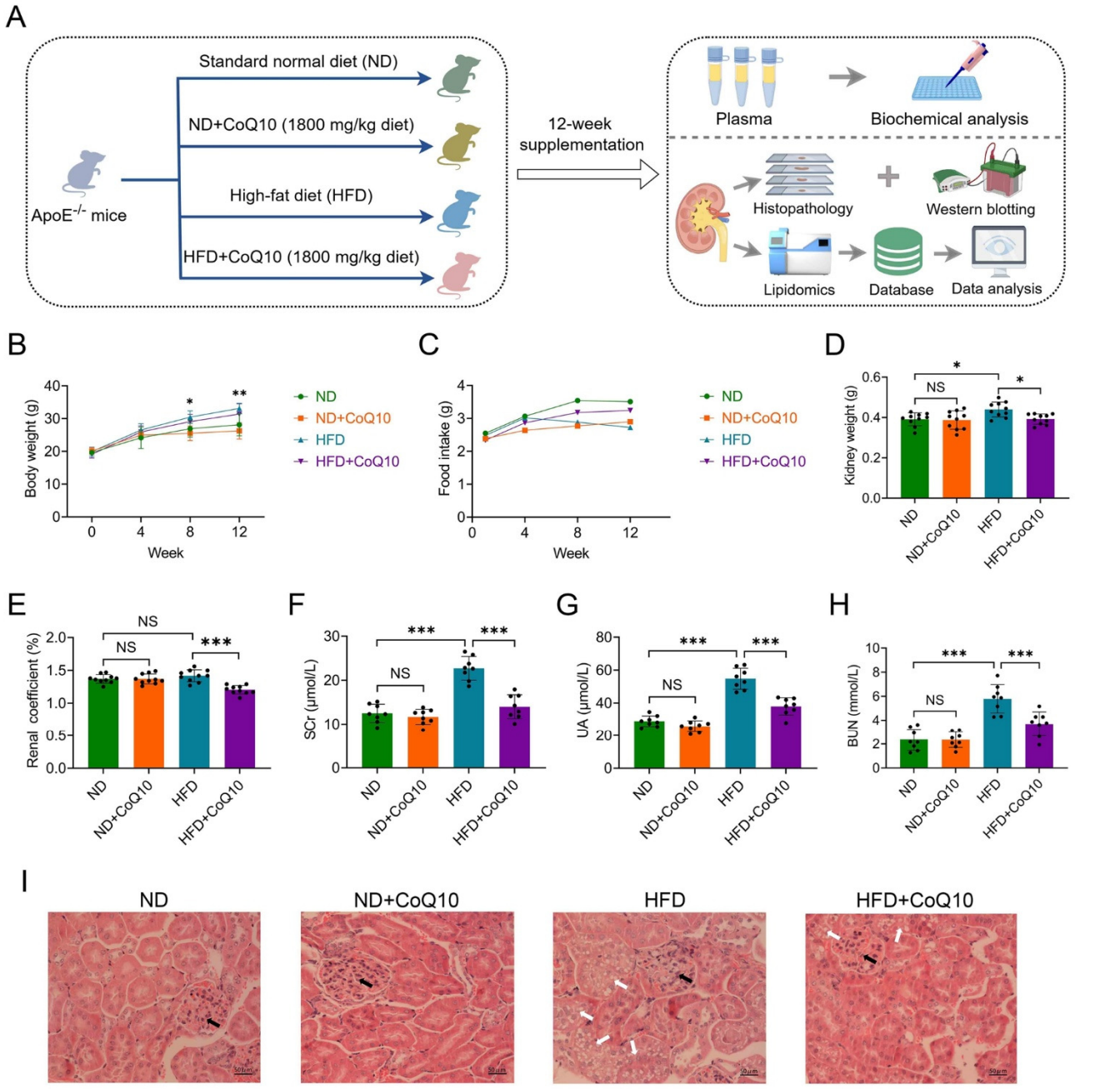

Fig. 1. CoQ10 alleviated renal injury in HFD-fed mice. (A) Flowchart of the experiments was shown. (B-C) The body weight of mice (B) and food intake (C) were monitored in the ND, ND+CoQ10, HFD and HFD+CoQ10 groups. *$P < 0.05$ and **$P < 0.01$: ND group *vs.* HFD group (n=10). (D) The weight of both kidneys was recorded in the end of 12 weeks of intervention (n=10). (E) The renal coefficient was indicated by kidney weight/body weight of mice (n=10). (F-H) The levels of SCr (F), serum UA (G) and BUN (H) were mearsured (n=8). In D-H, *$P < 0.05$, **$P < 0.01$ and ***$P < 0.001$; NS, not significant difference. (I) Representative images from HE staining of the kidney were presented (n=3).

3.2 CoQ10 prevented HFD-induced renal lipid accumulation and fibrosis

As illustrated in **Fig. 2A-2C**, a comparison with the ND mice reveals that HFD significantly increased lipid deposition in renal tissues by elevating levels of FFA, TC and TG. These effects were favorably attenuated by CoQ10 supplementation, suggesting that CoQ10 can effectively mitigate renal lipid deposition following 12 weeks of supplementation. Considering the established roles of peroxisome proliferators-activated receptor α (PPARα) and carnitine palmitoyltransferase 1A (CPT1A) in fatty acid oxidation, as well as AMP-activated protein kinase α2 (AMPKα2) and stearoyl-CoA desaturase (SCD) in lipid

synthesis[6], we investigated the impact of CoQ10 supplementation on these regulatory factors. CoQ10 significantly reversed HFD-induced reductions in AMPKα2 phosphorylation and expression, as well as CPT1A and PPARα expression, while downregulating HFD-elevated SCD expression **(Fig. 2D-2I)**. Additionally, Masson staining was used to assess fibrosis within the kidney tissue, revealing that collagen fiber deposition was significantly greater in HFD-fed mice compared to ND-fed mice **(Fig. 2J-2K)**. These detrimental changes induced by HFD were effectively alleviated by a 12-week CoQ10 supplementation **(Fig. 2J-2K)**. These data suggest that CoQ10 supplementation prevents HFD-induced renal lipid accumulation and fibrosis in hyperlipidemic ApoE$^{-/-}$ mice.

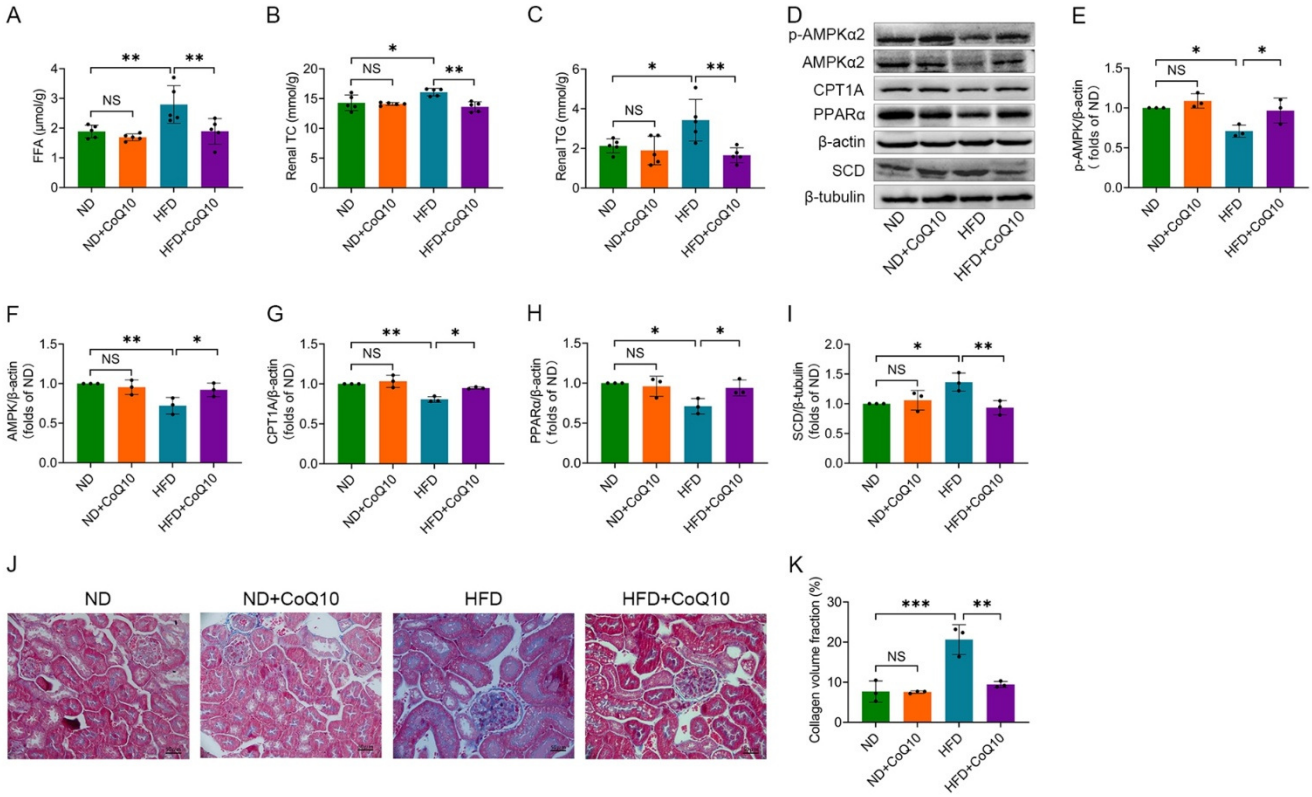

Fig. 2. CoQ10 prevented HFD-induced renal lipid accumulation and fibrosis. (A-C) The levels of FFA (A), TC (B) and TG (C) in the kidney were mearsured (n=5). (D) Representative bands of p-AMPKα2, AMPKα2, CPT1A, PPARα, and SCD proteins in the kidney from Western blot assays were presented. β-actin and β-tubulin were served as internal references. (E-I) The protein expression levels of p-AMPKα2, AMPKα2, CPT1A, PPARα, and SCD were analysed (n=3). (J-K) Representative images (J) and statistical analysis of collagen volume fraction (%) (K) from Masson staining of the kidney were presented (n=3). *$P < 0.05$, **$P < 0.01$ and ***$P < 0.001$.

3.3 CoQ10 attenuated HFD-induced renal oxidative stress and inflammation

We further determined the effect of CoQ10 supplementation on oxidative stress and inflammation within the kidney. As shown in **Fig. 3A**, HFD did not lead to a significant reduction in T-AOC levels in the kidney, although a trend towards a decreased effect was observed when compared to the ND group. After 12 weeks of CoQ10 supplementation, there was no significant increase in T-AOC levels in the HFD-fed mice. However, renal SOD activity levels, which were significantly decreased by HFD, were substantially restored following CoQ10 supplementation (**Fig. 3B**). Moreover, CoQ10 supplementation effectively attenuated the increase in MDA levels induced by HFD in the kidney **(Fig. 3C)**. Excessive lipid deposition leading to aberrant FAO contributes to mitochondrial dysfunction and results in inadequate ATP production[6]. As shown in **Fig. 3D**,

the insufficient ATP production induced by HFD was significantly reversed by CoQ10 supplementation in ApoE$^{-/-}$ mice. Additionally, Western blot analysis revealed that HFD feeding significantly upregulated the expression of pro-inflammatory cytokines IL-1β, IL-6, and TNF-α compared to the ND group, an effect markedly attenuated by CoQ10 supplementation **(Fig. 3E-3H)**. Consistently, CoQ10 significantly downregulated the HFD-induced increases in *IL-1β* and *IL-6* mRNA expression **(Fig. 3I-3J)**. However, CoQ10 intervention did not reverse the HFD-induced upregulation of *TNF-α* mRNA expression **(Fig. 3K)**. This suggests CoQ10 likely modulates TNF-α expression primarily at the post-transcriptional or translational level rather than transcriptionally, although this requires further investigation. Collectively, these findings demonstrate that CoQ10 supplementation alleviates HFD-induced renal oxidative stress and inflammation in ApoE$^{-/-}$ mice.

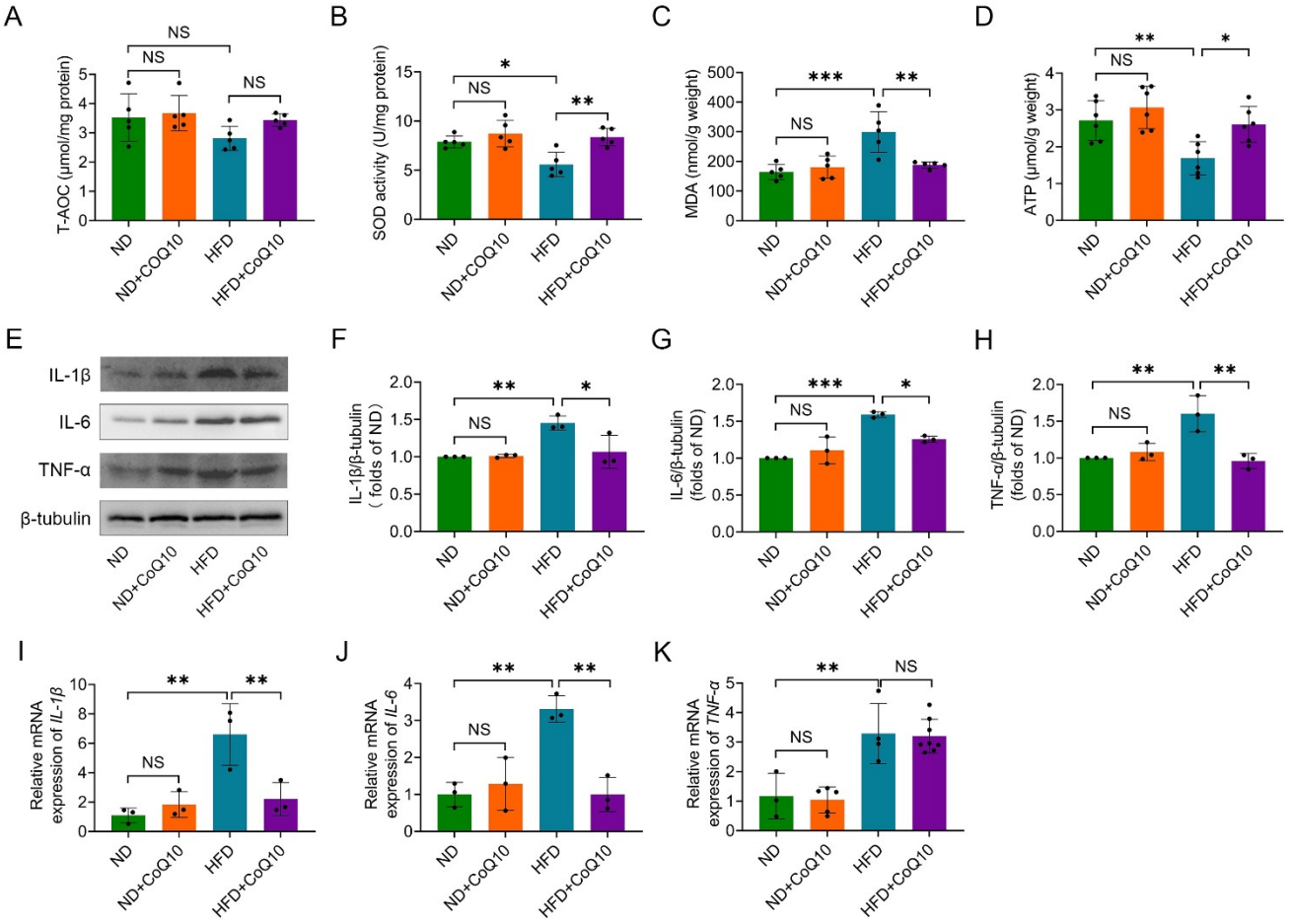

Fig. 3. CoQ10 attenuated HFD-induced renal oxidative stress and inflammation. (A-C) The levels of T-AOC (A), SOD activity (B), and MDA (C) in the kidney were determined (n=5). (D) The ATP levels in the kidney were measured (n=6). (E) Representative bands of IL-1β, IL-6, and TNF-α proteins in the kidney from Western blot were presented. β-tubulin was served as an internal reference. (F-H) The protein expression levels of IL-1β, IL-6, and TNF-α were analysed (n=3). (I-K) The relative mRNA expression levels of *IL-1β* (n=3), *IL-6* (n=3), and *TNF-α* (n=3-8) were determined. *$P < 0.05$, **$P < 0.01$ and ***$P < 0.001$; NS, not significant difference.

3.4 Untargeted lipidomic analysis of the kidneys

To further investigate alterations in renal lipid profiles in ApoE$^{-/-}$ mice, the renal lipid components were analyzed using UPLC-TOF/MS. After excluding ion features with a RSD greater than 30%, a total of 2529 lipid compounds were identified in the kidney samples, with 2060 compounds detected in ESI^{+} mode and 469

in ESI$^-$ mode. These compounds were categorized into 80 distinct subclasses and primarily classified into 8 superclasses: glycerophospholipids (GP, 47.17%), glycerolipids (GL, 22.62%), sphingolipids (SP, 15.34%), ether lipids (EL, 7.63%), fatty acyls (FA, 3.80%), sterol lipids (ST, 2.53%), glucosylsphingoshine (SoG, 0.47%), and prenol lipids (PR, 0.32%) **(Fig. 4A)**. Among the 80 distinct subclasses, the predominant species were phosphatidylcholines (PC, 24.95%), triglycerides (TG, 10.44%), and sphingomyelins (SM, 8.26%). The distribution of all lipid subclasses was depicted in **Supplementary Fig. S2**.

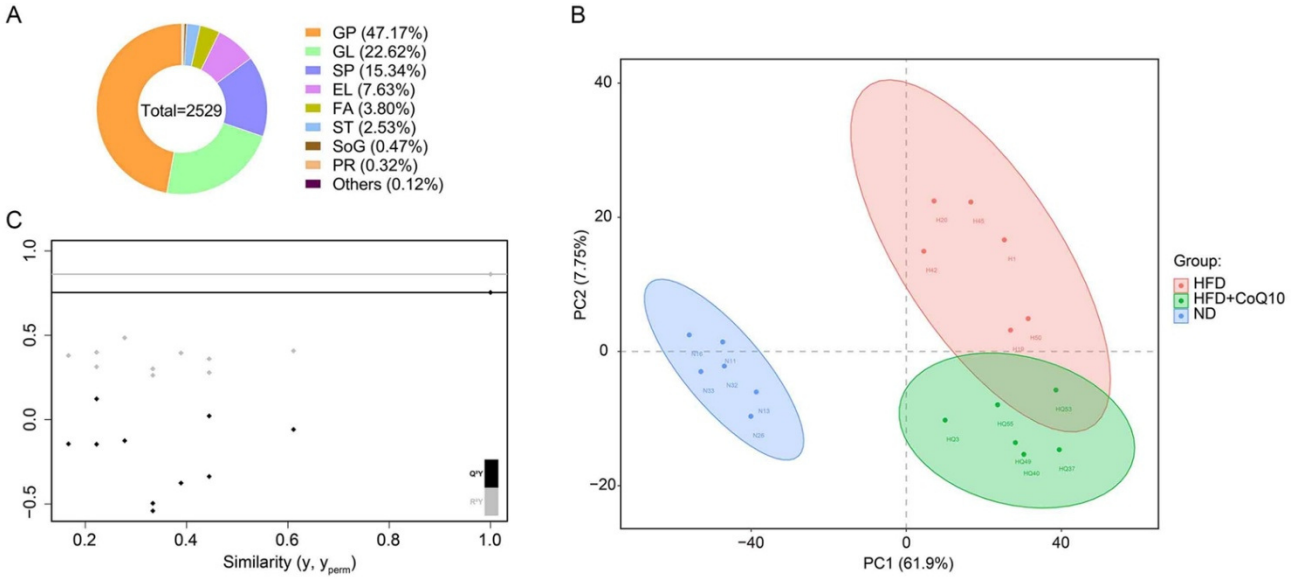

Fig. 4. Renal untargeted lipidomics analysis by UPLC-TOF/MS. (A) The percentage of lipid superclasses was shown. (B) The PLS-DA score plot of the ND, HFD and HFD+CoQ10 groups was shown. (C) The R^2Y and Q^2Y value in the PLS-DA model was presented.

To identify differential lipid biomarkers in renal tissue, PLS-DA was used to characterize metabolic profiles across the three experimental groups. The PLS-DA model accounted for 69.65% of total variance in the first two principal components (PC1 and PC2; **Fig. 4B**), with model validity metrics ($R^2Y = 0.86$, $Q^2Y = 0.75$) indicating robust explanatory power. Permutation testing confirmed no overfitting **(Fig. 4C)**. Additionally, the PLS-DA score plot showed a clear separation among ND, HFD, and HFD+CoQ10 groups, and tight intra-group clustering of biological replicates **(Fig. 4B)**. This demonstrates minimal inter-individual variation within treatment groups and pronounced lipidomic remodeling induced by HFD and modulated by CoQ10.

Differential lipids were identified through hierarchical clustering analysis using PLS-DA with VIP > 1.0 and FDR-corrected $P < 0.05$. A total of 878 differential lipids were identified among the ND, HFD and HFD+CoQ10 groups, which were annotated using KEGG and HMDB databases. The heat map of the different lipids identified among the three groups was shown in **Fig. 5A**. Volcano plots demonstrated that compared to ND group, HFD mice exhibited 528 upregulated and 305 downregulated lipids (**Fig. 5B**). CoQ10 intervention significantly modulated 126 lipids (90 upregulated and 36 downregulated) versus HFD group (**Fig. 5C**). In comparison to the ND group, the HFD group exhibited significant alterations in lipid profiles, with 143 GP upregulated and 132 downregulated, primarily involving PC, phosphatidylethanolamine (PE), and cardiolipin (CL). Additionally, there were 32 SP upregulated and 28 downregulated, mainly comprising

SM, as well as 24 GL upregulated and 4 downregulated, predominantly including TG and diacylglycerol (DG). Furthermore, when compared to the HFD group, the HFD+CoQ10 group demonstrated 16 downregulated and 25 upregulated GP, along with 6 downregulated and 1 upregulated SP. Differential lipid analysis was employed to generate KEGG classification maps and enrichment maps for the kidney, as depicted in **Fig. 5D**, which highlights the top 30 pathways based on *P* values. The HFD significantly impacted pathways related to GP metabolism, fat digestion and absorption, SP signaling pathway, autophagy, the phospholipase D signaling pathway, the cAMP signaling pathway, the phosphatidylinositol signaling system, the NFκB signaling pathway, among others. These pathways were favorably modulated by CoQ10 supplementation (**Fig. 5E**).

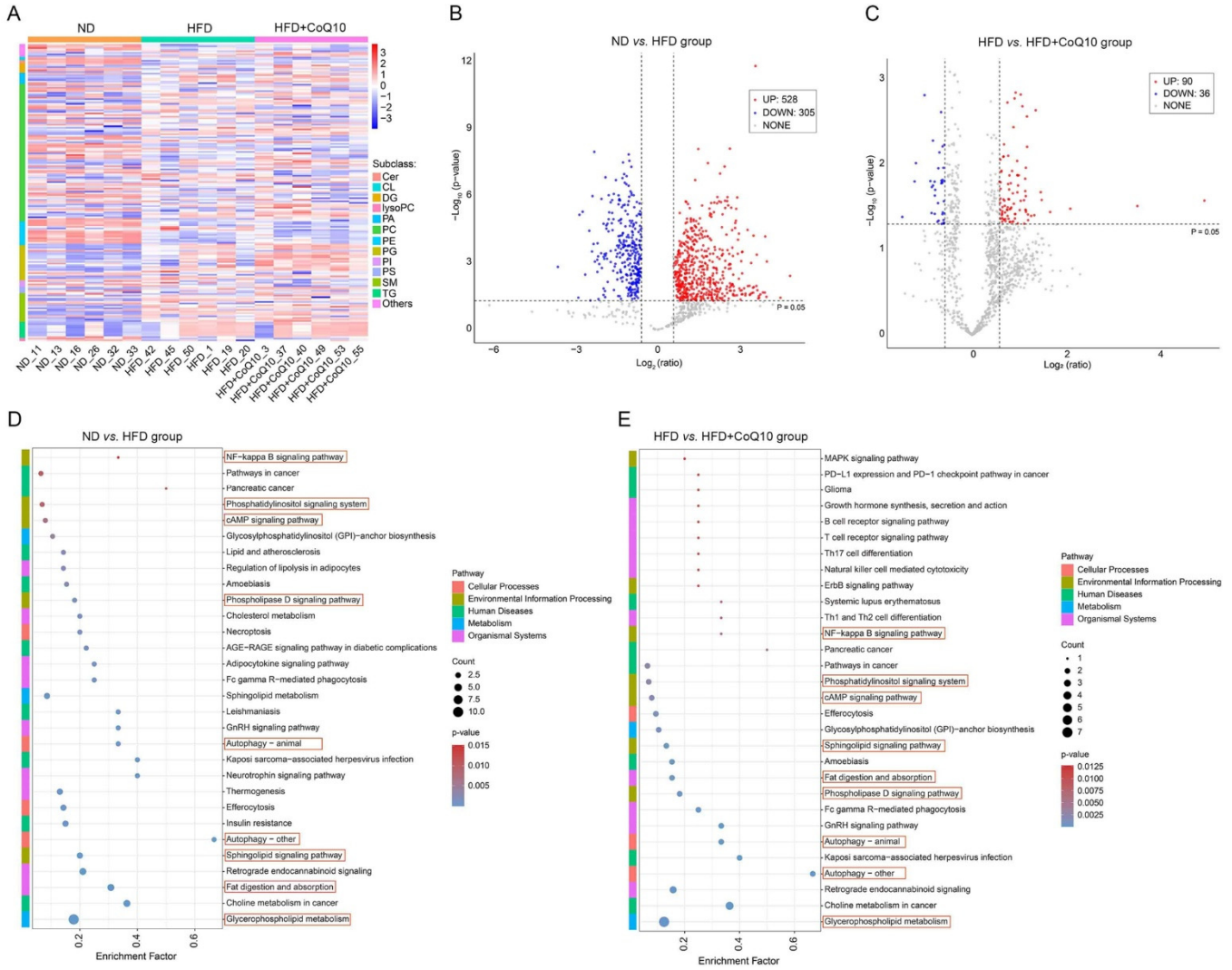

Fig. 5. Differential lipid species between the ND group and HFD group, and the HFD group and HFD+CoQ10 group according to the untargeted lipidomics analysis. (A) Heatmaps of pairwise comparison were shown. (B-C) Volcano plots for the ND group and HFD group (B), and for the HFD group and HFD+CoQ10 group (C) were shown. (D-E) KEGG enrichment analysis of the ND *vs.* HFD group (D), and the HFD *vs.* HFD+CoQ10 group (E) based on the differential lipids were presented. Signiffcantly enriched pathways were identiffed via the analysis of *P*-values and Rich Factor.

3.5 Targeted lipidomic analysis of glycerophospholipids within the kidneys

Based on the results from the untargeted lipidomic analysis, the KEGG pathway enrichment analysis identified GP metabolism as the most significantly enriched pathway. To obtain a more comprehensive understanding of lipid metabolism, GP was further examined by targeted lipidomic analysis using

UPLC-MS/MS. The ion peak of each sample was used to assess the stability of the instrument conditions, with each black point representing an individual sample. As shown in **Fig. 6A**, the PC1 scores fell within the range of plus or minus three standard deviations (3SD), indicating normal fluctuations. Moreover, the PLS-DA scores showed that PC1 and PC2 accounted for 66.5% of the variance **(Fig. 6B)**. Additionally, the interactive validation of the orthogonal partial least squares discriminant analysis (OPLS-DA) model demonstrated that the R^2Y and Q^2Y values for the HFD versus ND group were 0.998 and 0.943, respectively **(Fig. 6C)**, while for the HFD versus HFD+CoQ10 group, the values were 0.971 and 0.531, respectively **(Fig. 6D)**. These results suggest that the model is stable and reliable, without evidence of overfitting.

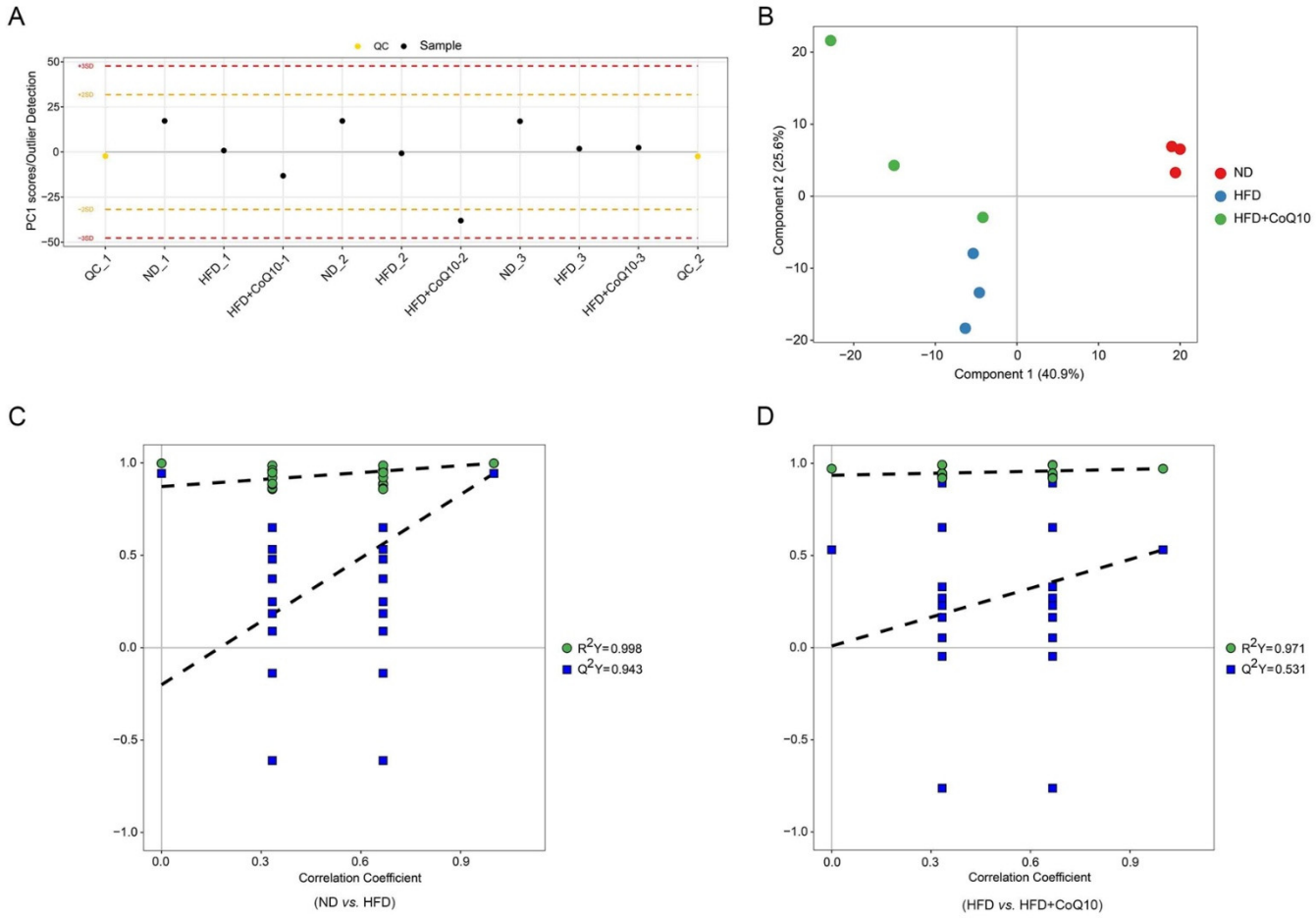

Fig. 6. Renal targeted lipidomic analysis of glycerophospholipids by UPLC-MS/MS. (A-B) PCA score plot of the ND, HFD and HFD+CoQ10 groups was shown. (C-D) The R^2Y and Q^2Y value in the PLS-DA model for the ND *vs.* HFD group (C), and the HFD *vs.* HFD+CoQ10 group (D) was presented.

A total of 631 lipids species, categorized into 17 distinct subclasses within the GP category, were identified across the ND, HFD and HFD+CoQ10 groups. Among these, the predominant subclasses were triacylglycerol (TAG, 32.74%), PE (32.65%), and PC (15.38%) **(Fig. 7A)**. Notable differences were observed among the three groups concerning the relative average abundance ratio of several lipid metabolites, including PE, CL, globotriaosylceramide (Gb3), phosphatidylinositol (PI), 1-alkyl,2-acylglycerophosphoinositols (PI_O), ganglioside (GM1), 1-alkenyl,2-acylglycerophosphoinositols (PI_P), ceramide phosphoethanolamines (CerPE), and 1-alkyl,2-acylglycerophosphatidylethanolamines (PE_O) **(Fig. 7B)**. The criteria of VIP $>$ 1 and P $<$ 0.05 was used to further analyze the differential lipids between the ND and

HFD groups, and between the HFD and HFD+CoQ10 groups. The volcano plot revealed 104 upregulated and 77 downregulated lipid metabolites in the HFD group compared to the ND group (**Fig. 7C, Supplementary Table S3)**. Additionally, in comparion to the HFD group, the HFD+CoQ10 group exhibited 10 upregulated and 23 downregulated metabolites **(Fig. 7D, Supplementary Table S4)**.

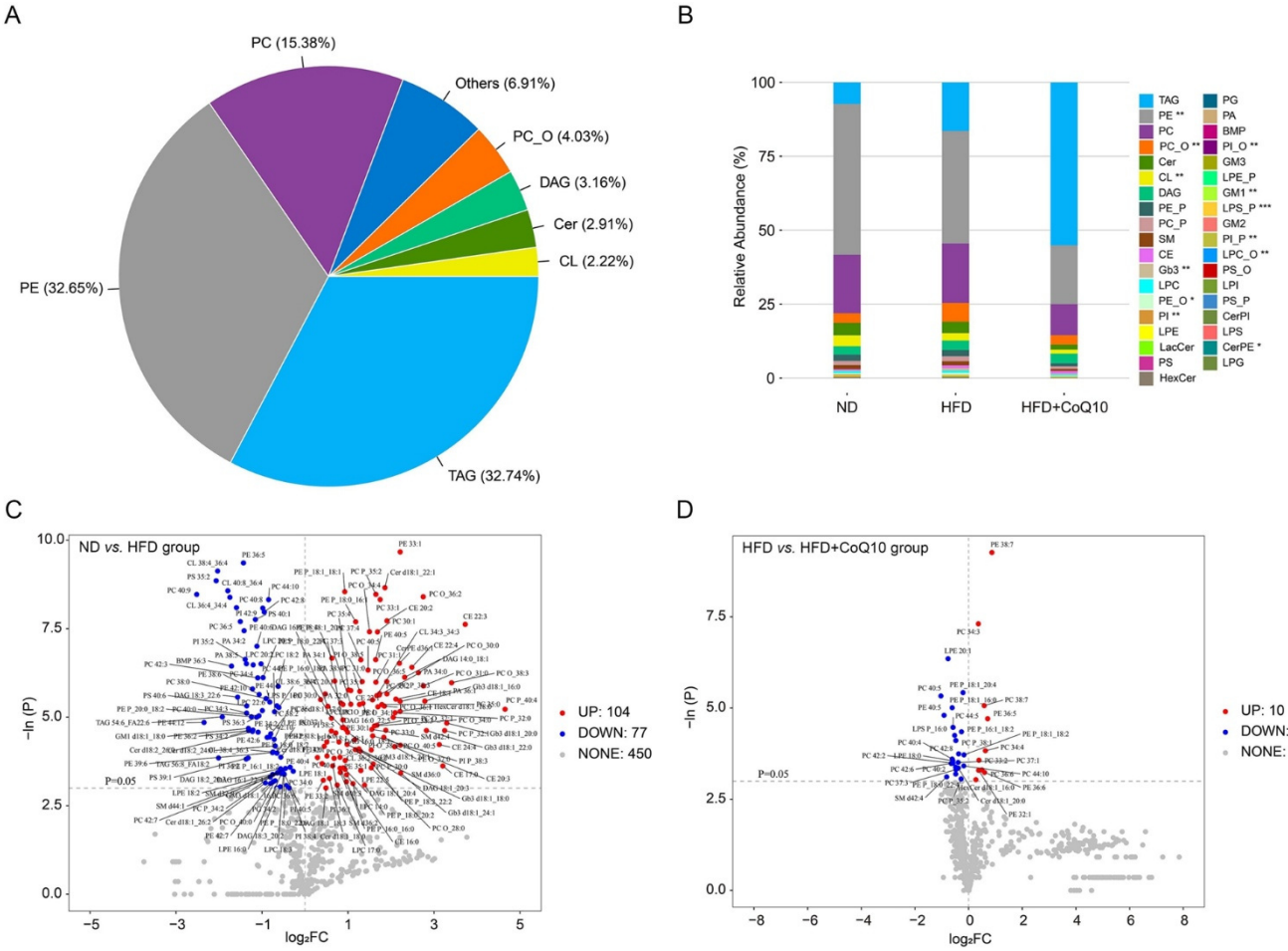

Fig. 7. The lipid categories and differential lipid species in glycerophospholipids were identiffed according to UPLC-MS/MS analysis. (A) The percentage of lipid subclasses in glycerophospholipids was shown. (B) The relative average abundance ratio of all lipid metabolites in the ND, HFD and HFD+CoQ10 groups was shown. (C-D) Volcano plots for the ND *vs.* HFD group (C), and for the HFD *vs.* HFD+CoQ10 group (D) were shown.

In particular, a HFD resutled in significant decreases in levels of renal PC species, specifically PC (34:4), PC (36:6), PC (42:1) and PC (42:10). CoQ10 supplementation greatly elevated the levels of PC (34:4) and PC (36:6) in the HFD-fed mice (**Fig. 8A**). Moreover, HFD induced an upregulation of various lipidomic metabolites in the kidney, including PC (40:5), PC (40:4), PC (37:3), PC (37:1), PC_O (38:3), phosphatidylethanolamine plasmalogen (PE_P) (18:0/22:4), PE (40:5), PE_P (18:1/16:0), PE_P (18:1/20:4), PC_P (35:2), and sphingomyelin (SM_d) (42:4). These lipid biomarkers were markedly downregulated in the HFD+CoQ10 group (**Fig. 8B, 8C, 8E, and 8F**). However, the decreased levels of renal lysophosphatidylcholine (LPC) and CL induced by HFD were not significantly altered by CoQ10 supplementation; these lipids included LPC (18:2), LPC (20:2), LPC (20:5), LPC (22:6), CL (38:4/36:3), CL (38:4/36:4), CL (40:8/36:4), and CL (36:4/34:4) (**Fig. 8D and 8G**). Furthermore, other major lipid species, such as PC (30:0), PC (37:4), PC (35:1), PC (33:1), PC_O (32:1), cholesterol ester (CE) (18:1), and PI (38:5), which were increased by HFD, were not significantly affected by CoQ10 supplementation (**Fig. S3**).

Finally, an analysis of correlations between differential lipids and biological parameters was conducted for the HFD+CoQ10 group. As shown in **Fig. 8H**, SOD activity levels demonstrated negative correlations with PE_P (18:1/16:0), SM_d (42:4), and FFA levels in the kidney. MDA levels showed significant positive correlations with PC_P (35:2), PE (40:5), and TG levels. Additionally, SCr levels were positively correlated with PE_P (18:1/16:0), SM_d (42:4), and FFA levels. UA levels were observed to exhibit significant positive correlations with PC (40:5) and FFA levels. Furthermore, BUN levels were positively associated with PC_P (35:2), PE (40:5), and TG levels. Conversely, ATP levels in the kidney were negatively correlated with PC (37:1) and PC (40:4) levels.

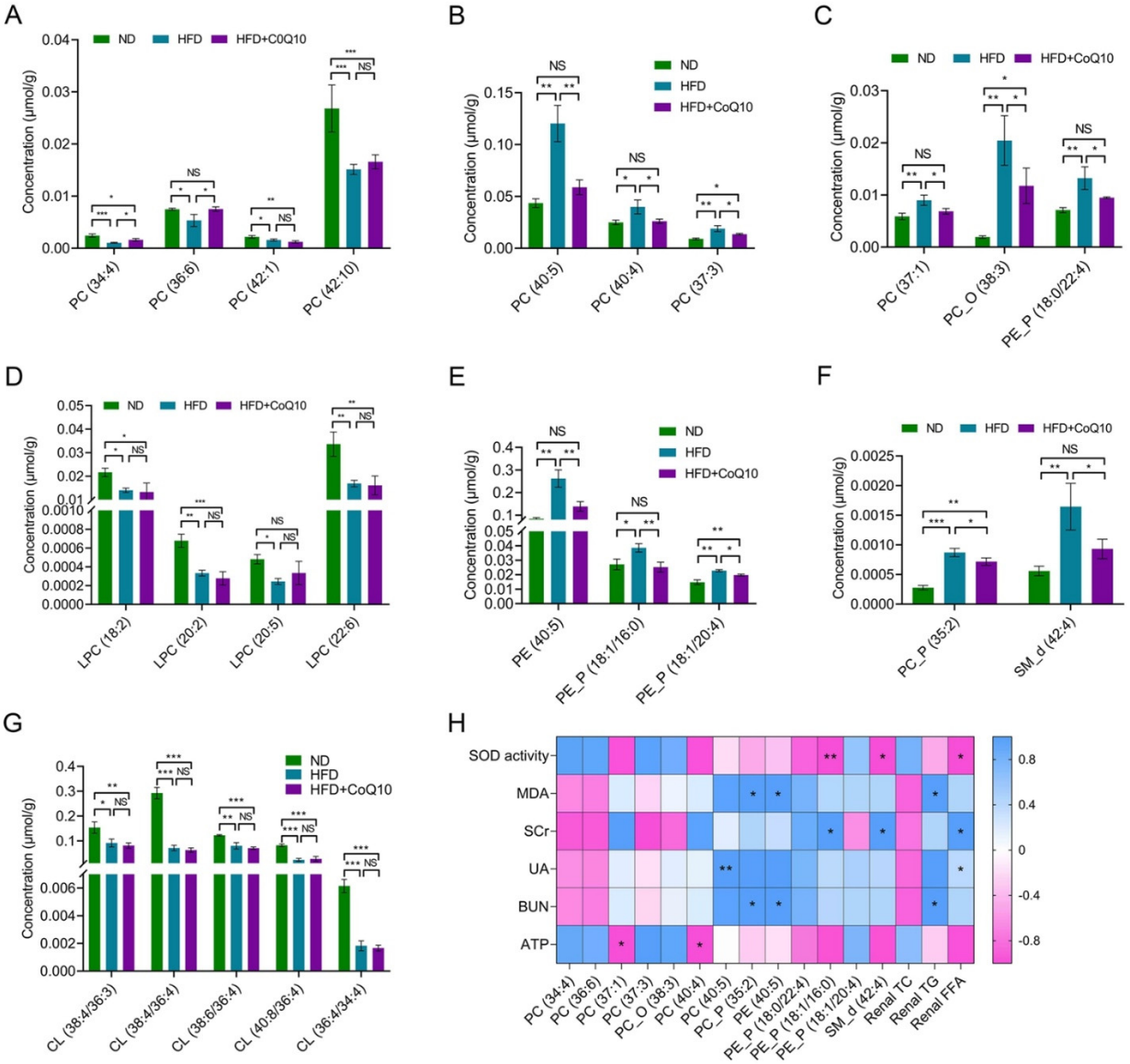

Fig. 8. Differential lipid species in glycerophospholipids among the ND, HFD and HFD+CoQ10 groups according to UPLC-MS/MS analysis. (A-G) Comparations of lipid concentration in the kidney among the ND, HFD and HFD+CoQ10 groups were shown. All data were assessed by a one-way ANOVA followed by Tukey's multiple comparisons test. *$P < 0.05$, **$P < 0.01$ and ***$P < 0.001$; NS, not significant difference (n=3). (H) Association between differential lipids and biological parameters was performed using Pearson's correlation analysis. *$P < 0.05$ and **$P < 0.01$ (n=3).

3.6 CoQ10 downregulated renal PI3K/Akt and TLR4/MyD88/NFκB signaling pathways in HFD-fed mice

Research has indicated that the PI3K/Akt and NFκB signaling pathways are crucial in modulating glucose and lipid metabolism during the progression of CKD [23]. In conjunction with KEGG analysis derived

from untargeted lipidomic data, we aim to investigate the involvement of PI3K/Akt and NFκB signaling in the mitigation of renal damage by CoQ10 in hyperlipidemic ApoE$^{-/-}$ mice. As shown in **Fig. 9A-9E**, HFD significantly increased the phosphorylation levels of PI3K and Akt in the kidney, which were favorably downregulated by CoQ10 supplementation. However, CoQ10 failed to significantly modulate PI3K and Akt expression in HFD-fed mice **(Fig. 9A-9E)**. The TLR4 receptor possesses a cytoplasmic signaling domain that recruits MyD88 to activate NFκB-mediated proinflammatory responses[24]. As shown in **Fig. 9F**, CoQ10 supplementation significantly downregulated the HFD-induced increase in renal *TLR4* mRNA expression. Western blot analysis further revealed that HFD markedly increased the renal protein expression of TLR4 and MyD88; however, this upregulation was substantially attenuated by CoQ10 supplementation **(Fig. 9G-9I)**. Additionally, CoQ10 significantly reversed the HFD-induced increases in NFκB p65 expression and phosphorylation **(Fig. 9J-9L)**. Activation of NFκB is initiated by the signal-induced phosphorylation of IκB, a key cytosolic inhibitor of NFκB, which triggers IκB ubiquitination and degradation. We further observed that CoQ10 supplementation reversed the HFD-mediated upregulation of IκB phosphorylation and consequent increase in IκB degradation **(Fig. 9J, 9M-9N)**. Notably, these biomarkers were not significantly modulated by CoQ10 in the ND-fed mice. Collectively, our findings demonstrate that 12 weeks of CoQ10 supplementation downregulate both the PI3K/Akt and TLR4/MyD88/NFκB signaling pathways in the kidneys of HFD-fed mice.

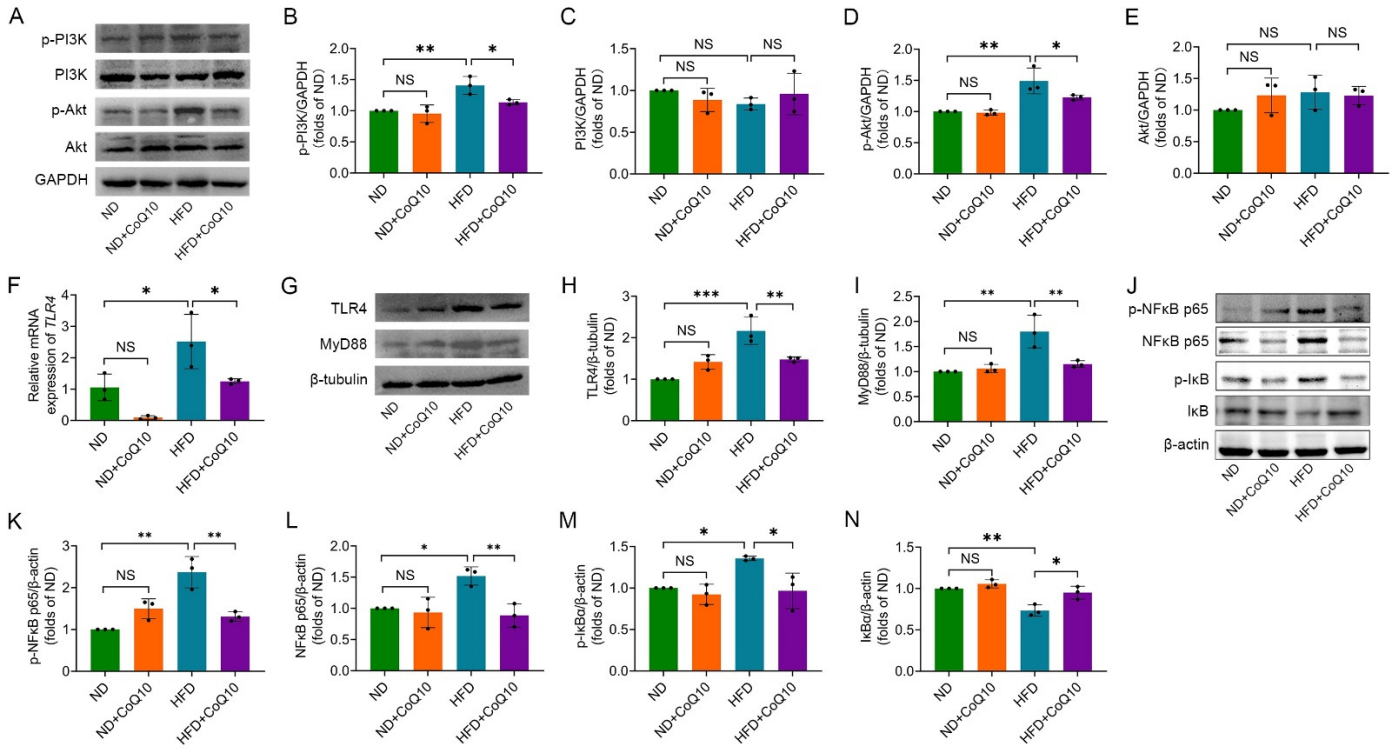

Fig. 9. CoQ10 downregulated renal PI3K/Akt and TLR4/MyD88/NFκB signaling pathways in HFD-fed mice. (A, G, J) Representative bands of p-PI3K, PI3K, p-Akt, Akt, TLR4, MyD88, p-NFκB p65, NFκB p65, p-IκB, and IκB in the kidney from Western blot were presented. GAPDH, β-actin and β-tubulin were served as internal references. The relative expression levels of p-PI3K (B), PI3K (C), p-Akt (D), Akt (E), TLR4 (H), MyD88 (I), p-NFκB p65 (K), NFκB p65 (L), p-IκB (M), and IκB (N) were analysed. (F) The relative mRNA expression levels of renal *TLR4* were determined. *$P < 0.05$, **$P < 0.01$ and ***$P < 0.001$; NS, not significant difference (n=3).

4. Discussion

Long-term HFD consumption induces dyslipidemia, leading to significant alterations in renal lipid accumulation, metabolism, and lipotoxicity. These changes play a central role in initiating and accelerating CKD progression[4]. As a well-established dietary supplement, CoQ10 possesses multifaceted biological effects, including modulation of glucose and lipid metabolism[13]. In the present study, we revealed that CoQ10 supplementation alleviated HFD-induced renal damage in ApoE$^{-/-}$ mice by attenuating renal oxidative stress, inflammation, lipid accumulation, and fibrosis. This renoprotective effect may occur through downregulation of PI3K/Akt and TLR4/MyD88/NFκB signaling pathways and restoration of lipid homeostasis. These findings elucidate potential mechanisms underlying CoQ10-mediated attenuation of renal injury in hyperlipidemic atherosclerotic mice.

Systemic lipid abnormalities manifest in early stages of CKD and actively contribute to its pathogenesis. Elevated circulating TG levels constitute independent risk factors for advanced CKD onset[25]. Notably, LDL-C undergoes structural modifications during CKD progression, with increased predominance of atherogenic small dense LDL (sdLDL) particles[26]. Consequently, lipid-lowering therapies represent potential strategies to delay CKD progression[5]. Consistent with prior studies[14, 17], we demonstrated that CoQ10 supplementation significantly improved circulating lipid profile in HFD-fed mice, including lowering plasma TG, TC, and LDL-C levels[15]. While reduced circulating HDL-C is an established risk factor for advanced CKD[25], CoQ10 supplementation, despite showing an upward trend, did not significantly increase HDL-C levels in our model[15]. This result was in line with previous clinical evidence[27]. Collectively, the efficacy of CoQ10 supplementation on ameliorating systemic dyslipidemia (particularly TC, TG, and LDL-C reduction) likely contributes to renal injury mitigation under hyperlipidemic conditions.

SCr, UA and BUN serve as key biochemical indicators of renal function, with elevated concentrations reflecting the severity of renal impairment. These biomarkers correlate strongly with renal lipid deposition, oxidative stress, and inflammation[28]. Previous studies have reported that CoQ10 restored SCr and BUN levels, indicating a protective role in renal damage[29]. Consistently, our results showed that HFD-increased SCr, UA and BUN were significantly reversed by CoQ10 supplementation. Notably, the decreased levels of these renal biomarkers mediated by CoQ10 positively correlated with decreased renal levels of multiple lipid metabolites. In addition, reduced renal TG, FFA, and other lipid metabolites following CoQ10 supplementation significantly correlated with increased SOD activity and decreased MDA levels. These findings indicate that the improvement of CoQ10 in renal lipid deposition may occur through attenuation of oxidative stress under hyperlipidemic condition.

Ectopic lipid deposition in the kidney mediated by HFD triggers inflammatory response[3]. Consequently, the inhibitory effects of CoQ10 supplementation on renal lipid deposition could result in the decreased inflammation. Additionally, diminished oxidative stress and inflammation contribute to restored lipid homeostasis and renal function[30, 31]. Our findings further revealed that CoQ10 supplementation counteracts HFD-induced impairments of lipid regulators such as AMPKα2, CPT1A, PPARα, and SCD. This aligned with prior evidence demonstrating CoQ10-mediated upregulation of FAO pathways[32] and

AMPK-dependent suppression of lipogenesis[17]. Given the established roles of PPARα and CPT1A in fatty acid oxidation, and of AMPKα2 and SCD in lipid synthesis[6], we propose that CoQ10 modulates renal lipid metabolism through simultaneously promoting lipid degradation and inhibiting lipid synthesis. Addionally, aberrant FAO resulting from excessive lipid deposition contributes to mitochondrial dysfunction and insufficient ATP production. This ATP deficit further exacerbates renal lipid accumulation through a pathological feedback loop in CKD[6]. As an essential mitochondrial electron carrier and cofactor for ATP synthesis, exogenous CoQ10 supplementation exhibits protective effects against renal mitochondrial dysfunction[33]. Our study confirms that CoQ10 significantly reversed HFD-induced ATP deficiency in ApoE$^{-/-}$ mice. Collectively, these findings suggest that CoQ10-mediated enhancement of FAO pathways may break this vicious cycle by restoring ATP production while simultaneously reducing oxidative stress and inflammatory.

Long-term consumption of HFD leads to significant lipid dysmetabolism linked to disease pathogenesis. While CKD-related dyslipidaemia is extensively studied, the role of kidney lipid metabolism in CKD progression is less understood. A recent trial found that CoQ10 supplementation significantly altered plasma lipids in CKD patients [34], but its impact on renal lipid metabolism remains unclear. Untargeted lipidomic analysis demonstrated that HFD increased major lipid classes like GP, SP, and GL. GP lipids such as PC and PE serve as potential biomarkers for metabolic syndrome[35], with elevated PE levels linked to severe insulin-resistant diabetes and increased risks of heart failure and kidney disease[36]. Different PC lipid species may have varying effects on renal function during CKD progression[37]. In the kidney, SM, a significant type of SP, plays a key role in maintaining podocyte stability and the function of the glomerular filtration barrier. Elevated levels of SM are associated with renal lipotoxicity, which promotes oxidative stress, inflammation, and fibrosis in CKD[38]. Furthermore, recent studies highlight interaction between SP-GL crosstalk in CKD, where ceramide-driven inflammation works synergistically with GL-induced oxidative stress to accelerate fibrosis. Targeting these pathways presents therapeutic potential for lipid-mediated nephropathies[39]. Our current findings suggest that by modulating PC, PE, and SM, CoQ10 can ameliorate the imbalance between lipid synthesis and catabolism induced by a HFD, thereby exerting a protective effect against renal injury under hyperlipidemic conditions.

To further elucidate the regulatory mechanisms of renal function through CoQ10 supplementation, a targeted lipidomic analysis of GP was conducted in renal tissues using UPLC-MS/MS. PC represent the most abundant class of GP in cells and fulfill numerous functional roles. Reduced serum levels of PCs have been documented in rats with CKD[37]. Additionally, aberrant PC metabolism has been observed in patients with mild to advanced CKD[40]. Distinct PC species in circulation may exert differential effects on renal function during the CKD progression[37, 41]. For instance, elevated plasma levels of PC (30:1), PC (34:1), and PC (38:2) have been significantly correlated with an increased risk of all-cause mortality[42]. In contrast, CKD patients exhibit lower serum levels of PC (36:0), PC (44:3), and PC (48:0) compared to healthy controls, while serum levels of PC (40:2) and PC (46:0) are elevated[41]. Furthermore, plasma levels of PC (32:1), PC (34:1), PC

(38:8), PC (42:1), PC (42:8), and PC (42:11) are diminished in CKD-afflicted rats[37]. Despite these findings, the implications of disrupted renal PC metabolism on renal function under hyperlipidemic conditions remain inadequately dunderstood. Our current findings indicate that a HFD adversely modulates various PC species in the kidney, including upregulating PC (34:4) and PC (36:6) levels while downregulating PC (40:5), PC (40:4), PC (37:3), and PC (37:1) levels in HFD-fed mice. The observed improvement in renal PC metabolism mediated by CoQ10 may underlie its protective effect against renal injury in hyperlipidemic mice.

PE are zwitterionic phospholipids prevalent in cellular membranes and play crucial roles in maintaining membrane integrity, mitochondrial function, and lipid homeostasis. However, elevated PE levels have been prospectively linked to a more rapid decline in kidney function in patient with type 2 diabetes[43]. Additionally, the acyl-chain profiles of PE become progressively longer and more unsaturated with increasing CKD severity, with higher levels of polyunsaturated PE independently associated with an increased risk of diabetic kidney disease (DKD) progression[44]. Our study demonstrated that the HFD-increased renal unsaturated PE levels, such as PE (40:5), and their vinyl ether forms, including PE_P (18:0/22:4), PE_P (18:1/16:0), and PE_P (18:1/20:4), were favorably downregulated by CoQ10 supplementation. Aberrant PE composition and metabolism disrupt cellular function, increasing oxidative stress and inflammation[45]. Modulating CoQ10 in PE metabolism can protect against HFD-induced kidney injury in mice. LPC is a glycerophospholipid produced phospholipase A_2 (PLA_2) through the hydrolysis of PC into LPC and arachidonic acid. Reduced plasma levels of LPC species, such as LPC (18:2), LPC (20:3), and LPC (20:4), in patients at various stages of CKD[46, 47]. Additionally, disrupted CL content and composition result in mitochondrial dysfunction, increased oxidative stress, and cellular apoptosis[48]. In alignment with these findings, the present study revealed that HFD reduced the levels of several LPC and CL species in the kidney. Notably, however, CoQ10 supplementation did not significantly restore LPC and CL levels.

The differential modulation between PC/PE and LPC/CL likely reflects the metabolic compartmentalization and functional hierarchy within lipid pathways. The PC and PE biosynthesis via the endoplasmic reticulum-localized Kennedy pathway is regulated by CTP:phosphocholine cytidylyltransferase (CCTα), an enzyme known for its role as a redox sensor and its dependence on ATP[49]. The enhancement of mitochondrial oxidative phosphorylation mediated by CoQ10 leads to an increase in cytosolic ATP/ADP ratios and a reduction in oxidative stress[50], thereby establishing an optimal microenvironment for the activation of CCTα. This phenomenon accounts for the preferential modulation of PC and PE. Conversely, the dynamics of LPC are governed by the equilibrium between PLA_2-mediated hydrolysis of PC and the re-acylation cycles. Although currently unknown, the stability of LPC pools suggests that CoQ10 does not significantly disrupt this equilibrium, possibly due to the compensatory activation of LPC acyltransferases. Furthermore, the synthesis of CL necessitates enzymes encoded by mitochondrial DNA and specialized acyl chains provided by localized transacylation reactions[51]. These topological constraints may protect CL from systemic metabolic changes induced by CoQ10 supplementation. We propose that this selectivity reflects a functional adaptation, wherein CoQ10 enhances membrane biogenesis through PC and PE to support

organelle expansion during metabolic reprogramming, while maintaining the integrity of signaling lipids (LPC) and structural lipids (CL) that operate under distinct homeostatic regimes. Future studies involving the manipulation of key regulatory nodes, such as CCTα knockdown or Tafazzin overexpression, will further elucidate these mechanisms. While elucidating the precise molecular switches governing this selectivity requires further investigation, our work establishes CoQ10 as a topological regulator of lipid metabolism with preference for structurally critical phospholipid pathways.

The findings of the KEGG pathway enrichment analysis in this study suggest the involvement of PI3K/Akt and NFκB signaling pathways in aberrant lipid metabolism and renal damage induced by a HFD. The hyperactivation of these pathways is crucial in regulating lipid metabolism, oxidative stress injury, and inflammatory responses during the progression of CKD [23]. Consequently, we conducted experimental investigations to assess the effects of CoQ10 supplementation on these pathways. Our results demonstrated that CoQ10 supplementation significantly downregulated the PI3K/Akt and NFκB signaling activated by HFD, indicating a protective effect of CoQ10 against renal injury in hyperlipidemic mice. Furthermore, Akt phosphorylates IKKβ, enhancing NFκB activation and establishing a vicious cycle that links oxidative stress and inflammation[52]. Nevertheless, the interaction between the PI3K/Akt and NFκB signaling pathways in the ameliorative effects of CoQ10 on renal injury warrants further investigation.

Additionally, long-term HFD can stimulate TLR4 activation, which recruits MyD88 and activates the NFκB signaling pathway, leading to upregulation of proinflammatory cytokines such as IL-1β, IL-6 and TNF-α at both the mRNA and protein levels[24]. Inhibiting TLR4/NFκB signaling can alleviate renal inflammatory responses in a diabetic nephropathy[53]. In the present study, CoQ10 supplementation significantly downregulated both mRNA and protein expression of TLR4, as well as MyD88 protein expression in HFD-fed mice. These results suggest that suppression of the TLR4/MyD88/NFκB signaling mediates the alleviation of renal injury by CoQ10 in hyperlipidemic ApoE$^{-/-}$ mice. Nevertheless, the precise role of the TLR4/MyD88/NFκB signaling pathway in modulating renal lipid metabolism under hyperlipidemic conditions remains unclear and warrants further investigation. Furthermore, as TLR4 acts upstream of both the PI3K/Akt and NFκB pathways, future studies employing TLR4 knockout mice or human renal cell lines should elucidate the specific contribution of TLR4 to CoQ10's renoprotective effects in hyperlipidemia.

Extensive clinical evidence supports the safety and therapeutic potential of CoQ10 supplementation in renal disease. Human studies have consistently demonstrated the safety of CoQ10 administration at doses up to 1200 mg/day, with accumulating evidence suggesting its renoprotective effects in CKD[16]. Clinical trials have indicated that a 6-week supplementation regimen of 1200 mg/day CoQ10 significantly ameliorated oxidative stress, inflammation, and cellular bioenergetics in patients with moderate-to-severe CKD[54]. Similarly, patients with diabetic nephropathy who receivinged 150 mg/day CoQ10 for 12 weeks exhibited significant improvements in glycemic control, oxidative stress parameters, and inflammatory biomarkers[55, 56]. Despite these promising findings, the efficacy of CoQ10 in specifically addressing

hyperlipidemia-associated CKD remains to be established. Therefore, we propose that future randomized controlled trials should investigate the protective potential of CoQ10 supplementation in high-risk populations with concurrent hyperlipidemia and CVDs, with a particular focus on its long-term renal protective effects.

Despite its potential advantages, CoQ10 demonstrates limited oral bioavailability, typically less than 5%, primarily attributed to its substantial molecular weight (863 Da) and lipophilic nature. Upon ingestion, CoQ10 is predominantly absorbed in the small intestine through chylomicron-mediated transport, with peak plasma concentrations occurring approximately six hours post-administration[57]. The bioavailability of CoQ10 is significantly influenced by factors such as formulation design (e.g., nanoemulsions or crystalline structures), chemical form (ubiquinol or ubiquinone), and dietary context[58]. Following absorption, CoQ10 is incorporated into very-low-density lipoproteins (VLDLs) in the liver for systemic distribution. Tissue uptake of CoQ10 is organotropic, with the highest accumulation observed in cardiac tissue, moderate levels in the kidneys and liver, and a preferential subcellular localization, with 40%–50% localizing to mitochondrial membranes[50]. Notably, more than 95% of circulating CoQ10 exists in the reduced form, which reflects its redox buffering capacity in plasma[59]. The compound undergoes continuous redox cycling without hepatic metabolism, with elimination primarily occurring through biliary excretion, accounting for over 90% fecal elimination. Renal clearance is minimal (less than 1%), due to extensive protein binding and physicochemical constraints[57]. In our HFD-fed ApoE$^{-/-}$ model, a 12-week supplementation with CoQ10 at a dosage of 1800 mg/kg diet resulted in plasma concentrations of (3.196 ± 0.511) μmol/L[15], which fall within the protective range shown to enhance renal function in clinical studies[16]. Future research should investigate the dose-response relationships of CoQ10 supplementation in models of hyperlipidemia-induced renal injury to determine optimal dosing regimens.

5. Conclusion

In summary, our research establishes a novel direct association between CoQ10 supplementation and renal function in the context of hyperlipidemic conditions. Our results demonstrate that CoQ10 significantly mitigates HFD-induced renal damage in ApoE$^{-/-}$ mice by reducing oxidative stress, inflammation, and lipid accumulation in the kidneys, potentially through mechanisms involving the modulation of lipid metabolism. Given that HFD-induced CKD is closely linked with increased atherosclerosis and cardiovascular disease risk, and considering our previous studies indicating a protective effect of CoQ10 against atherosclerosis and CVDs[14, 15], these findings offer new insights into the protective role of CoQ10 against renal injury and atherothrombosis under hyperlipidemic conditions.

Conflict of interest statement

None.

Acknowledgements

This work was supported by the National Natural Science Foundation of China (grant No. 82260638) and Yunnan Fundamental Research Projects (202401AT070081).

References

[1] A. Francis, M. N. Harhay, A. C. M. Ong, et al., Chronic kidney disease and the global public health agenda: an international consensus, Nat. Rev. Nephrol. 20 (2024) 473-485. https://doi.org/10.1038/s41581-024-00820-6.

[2] C. W. Fwu, I. H. Schulman, J. M. Lawrence, et al., Association of Obesity, Metabolic Syndrome, and Diabetes With Urinary Incontinence and Chronic Kidney Disease: Analysis of the National Health and Nutrition Examination Survey, 2003-2020, J. Urol. 211 (2024) 124-133. https://doi.org/10.1097/JU.0000000000003761.

[3] J. Baek, C. He, F. Afshinnia, et al., Lipidomic approaches to dissect dysregulated lipid metabolism in kidney disease, Nat. Rev. Nephrol. 18 (2022) 38-55. https://doi.org/10.1038/s41581-021-00488-2.

[4] S. H. Suh and S. W. Kim, Dyslipidemia in Patients with Chronic Kidney Disease: An Updated Overview, Diabetes Metab. J. 47 (2023) 612-629. https://doi.org/10.4093/dmj.2023.0067.

[5] C. J. Ferro, P. B. Mark, M. Kanbay, et al., Lipid management in patients with chronic kidney disease, Nat. Rev. Nephrol. 14 (2018) 727-749. https://doi.org/10.4093/dmj.2023.0067.

[6] A. Mitrofanova, S. Merscher, and A. Fornoni, Kidney lipid dysmetabolism and lipid droplet accumulation in chronic kidney disease, Nat. Rev. Nephrol. 19 (2023) 629-645. https://doi.org/10.1038/s41581-023-00741-w.

[7] Z. Gao and X. Chen, Fatty Acid beta-Oxidation in Kidney Diseases: Perspectives on Pathophysiological Mechanisms and Therapeutic Opportunities, Front. Pharmacol. 13 (2022) 805281. https://doi.org/10.3389/fphar.2022.805281.

[8] S. E. Piret, A. A. Attallah, X. Gu, et al., Loss of proximal tubular transcription factor Kruppel-like factor 15 exacerbates kidney injury through loss of fatty acid oxidation, Kidney Int. 100 (2021) 1250-1267. https://doi.org/10.1016/j.kint.2021.08.031.

[9] B. Cong, Perspectives in Food & Medicine Homology. Food Med. Homol. 1 (2024) 9420018. https://doi.org/10.26599/FMH.2024.9420018

[10] P. Ma, L. Zhang, Z. Wang, et al., Black tea extract ameliorates fatty liver and fatty kidney in HFD-induced obese mice. Food Sci. Hum. Wellness. 2024. https://doi.org/10.26599/FSHW.2024.9250391

[11] T. A. Ikizler, J. D. Burrowes, L. D. Byham-Gray, et al., KDOQI Clinical Practice Guideline for Nutrition in CKD: 2020 Update, Am. J. Kidney Dis. 76 (2020) S1-S107. https://doi.org/ j.ajkd.2020.05.006.

[12] K. Lambert, R. Gardos, H. Coolican, et al., Diet and Polycystic Kidney Disease: Nutrients, Foods, Dietary Patterns, and Implications for Practice, Semin. Nephrol. 43 (2023) 151405. https://doi.org/10.1016/j.semnephrol.2023.151405.

[13] M. Arenas-Jal, J. M. Sune-Negre, and E. Garcia-Montoya, Coenzyme Q10 supplementation: Efficacy, safety, and formulation challenges, Compr. Rev. Food Sci. Food Saf. 19 (2020) 574-594. https://doi.org/10.1111/1541-4337.12539.

[14] F. Ya, X. R. Xu, Y. Shi, et al., Coenzyme Q10 Upregulates Platelet cAMP/PKA Pathway and Attenuates Integrin alphaIIbbeta3 Signaling and Thrombus Growth, Mol. Nutr. Food Res. 63 (2019) e1900662. https://doi.org/10.1002/mnfr.201900662.

[15] F. Ya, X. R. Xu, Z. Tian, et al., Coenzyme Q10 attenuates platelet integrin alphaIIbbeta3 signaling and platelet hyper-reactivity in ApoE-deficient mice, Food Funct. 11 (2020) 139-152. https://doi.org/10.1039/c9fo01686d.

[16] Y. Xu, G. Yang, X. Zuo, et al., A systematic review for the efficacy of coenzyme Q10 in patients with chronic kidney disease, Int. Urol. Nephrol. 54 (2022) 173-184. https://doi.org/10.1007/s11255-021-02838-2.

[17] K. Chen, X. Chen, H. Xue, et al., Coenzyme Q10 attenuates high-fat diet-induced non-alcoholic fatty liver disease through activation of the AMPK pathway, Food Funct. 10 (2019) 814-823. https://doi.org/10.1039/c8fo01236a.

[18] D. Wang, X. Yan, M. Xia, et al., Coenzyme Q10 promotes macrophage cholesterol efflux by regulation of the activator protein-1/miR-378/ATP-binding cassette transporter G1-signaling pathway, Arterioscler. Thromb. Vasc. Biol. 34 (2014) 1860-1870. https://doi.org/10.1161/ATVBAHA.113.302879.

[19] L. Cao, Y. Wu, K. Liu, et al., Cornus officinalis vinegar alters the gut microbiota, regulating lipid droplet changes in nonalcoholic fatty liver disease model mice. Food Med. Homol. 1 (2024) 9420002. https://doi.org/10.26599/FMH.2024.9420002

[20] Y. Liu, N. Ling, B. Zhang, et al., Flavonoid-Rich mulberry leaf extract modulate lipid metabolism, antioxidant capacity, and gut microbiota in high-fat diet-induced obesity: potential roles of FGF21 and SOCS2. Food Med. Homol. 1 (2024) 9420016. https://doi.org/10.26599/FMH.2024.9420016

[21] W. Li, C. Wu, X. Zhou, et al., Sulforaphane Attenuates CD36-mediated Platelet Hyperreactivity through Modulating cAMP/PKA/NOX2 Signaling in Hyperlipidemic Conditions. Food Sci. Hum. Wellness, 14 (2025) 9250165. https://doi.org/10.26599/FSHW.2024.9250165.

[22] Y. Ma, J. Hu, X. Bi, et al., Panax Notoginseng Saponins Attenuate Oxidative Stress-mediated Platelet Apoptosis in Hyperlipidemic Conditions via Up-regulating cAMP/PKA Signaling Pathway in vitro and in vivo. J. Future Foods, 2025. https://doi.org/10.1016/j.jfutfo.2024.11.016

[23] Q. Feng, X. Yu, J. Xie, et al., Phillygenin improves diabetic nephropathy by inhibiting inflammation and apoptosis via regulating TLR4/MyD88/NF-kappaB and PI3K/AKT/GSK3beta signaling pathways, Phytomedicine. 136 (2025) 156314. https://doi.org/10.1016/j.phymed.2024.156314.

[24] T. Bao, L. Ren, L. Qi, et al., Dual-immunomodulatory effects on RAW264.7 macrophages and structural elucidation of a polysaccharide isolated from fermentation broth of *Paecilomyces hepiali*, J. Future Foods, 5 (2025) 628-640. https://doi.org/10.1016/j.jfutfo.2024.11.010.

[25]M. Weldegiorgis and M. Woodward, Elevated triglycerides and reduced high-density lipoprotein cholesterol are independently associated with the onset of advanced chronic kidney disease: a cohort study of 911,360 individuals from the United Kingdom, BMC Nephrol. 23 (2022) 312. https://doi.org/10.1186/s12882-022-02932-2.

[26] Q. Yang, Y. Zou, Y. Lang, et al., Estimated small dense low-density lipoprotein-cholesterol and the risk of kidney and cardiovascular outcomes in diabetic kidney disease, Ren. Fail. 46 (2024) 2369701. https://doi.org/10.1080/0886022X.2024.2369701.

[27] P. Zhang, C. Yang, H. Guo, et al., Treatment of coenzyme Q10 for 24 weeks improves lipid and glycemic profile in dyslipidemic individuals, J. Clin. Lipidol. 12 (2018) 417-427 e5. https://doi.org/10.1016/j.jacl.2017.12.006.

[28] D. J. van Veldhuisen, L. M. Ruilope, A. S. Maisel, et al., Biomarkers of renal injury and function: diagnostic, prognostic and therapeutic implications in heart failure, Eur. Heart J. 37 (2016) 2577-2585. https://doi.org/10.1093/eurheartj/ehv588.

[29] E. K. Ozer, M. T. Goktas, I. Kilinc, et al., Coenzyme Q10 improves the survival, mesenteric perfusion, organs and vessel functions in septic rats, Biomed. Pharmacother. 91 (2017) 912-919. https://doi.org/10.1016/j.biopha.2017.05.017.

[30] H. H. Szeto, S. Liu, Y. Soong, et al., Protection of mitochondria prevents high-fat diet-induced glomerulopathy and proximal tubular injury, Kidney Int. 90 (2016) 997-1011. https://doi.org/10.1016/j.kint.2016.06.013.

[31] H. M. Kang, S. H. Ahn, P. Choi, et al., Defective fatty acid oxidation in renal tubular epithelial cells has a key role in kidney fibrosis development, Nature medicine 21 (2015) 37-46. https://doi.org/10.1016/j.kint.2016.06.013.

[32] S. Chokchaiwong, Y. T. Kuo, S. H. Lin, et al., Coenzyme Q10 serves to couple mitochondrial oxidative phosphorylation and fatty acid beta-oxidation, and attenuates NLRP3 inflammasome activation, Free Radic. Res. 52 (2018) 1445-1455. https://doi.org/10.1080/10715762.2018.1500695.

[33] K. C. Sourris, B. E. Harcourt, P. H. Tang, et al., Ubiquinone (coenzyme Q10) prevents renal mitochondrial dysfunction in an experimental model of type 2 diabetes, Free Radic. Biol. Med. 52 (2012) 716-723. https://doi.org/10.1016/j.freeradbiomed.2011.11.017.

[34] A. Ahmadi, G. Begue, A. P. Valencia, et al., Randomized crossover clinical trial of coenzyme Q10 and nicotinamide riboside in chronic kidney disease, JCI Insight 8 (2023) e167274. https://doi.org/10.1172/jci.insight.167274.

[35] Z. Yu, L. Fan, F. Tai, et al., Yolk free egg substitute improves the serum phospholipid profile of mice with metabolic syndrome based on lipidomic analysis. Food Sci. Hum. Wellness. 13 (2024) 482-493. https://doi.org/10.26599/FSHW.2022.9250042

[36] J. Wang, J. J. Liu, R. L. Gurung, et al., Clinical variable-based cluster analysis identifies novel subgroups with a distinct genetic signature, lipidomic pattern and cardio-renal risks in Asian patients with recent-onset type 2 diabetes, Diabetologia 65 (2022) 2146-2156. https://doi.org/10.1007/s00125-022-05741-2.

[37] Y. N. Wang, Z. H. Zhang, H. J. Liu, et al., Integrative phosphatidylcholine metabolism through phospholipase A_2 in rats with chronic kidney disease, Acta Pharmacol. Sin. 44 (2023) 393-405. https://doi.org/10.1038/s41401-022-00947-x.

[38] D. Pongrac Barlovic, V. Harjutsalo, N. Sandholm, et al., Sphingomyelin and progression of renal and coronary heart disease in individuals with type 1 diabetes, Diabetologia 63 (2020) 1847-1856. https://doi.org/10.1007/s00125-020-05201-9.

[39] Z. Sakic, A. Atic, S. Potocki, et al., Sphingolipids and Chronic Kidney Disease, J. Clin. Med. 13 (2024) 5050. https://doi.org/10.3390/jcm13175050.

[40] E. Nkuipou-Kenfack, F. Duranton, N. Gayrard, et al., Assessment of metabolomic and proteomic biomarkers in detection and prognosis of progression of renal function in chronic kidney disease, PloS one 9 (2014) e96955. https://doi.org/10.1371/journal.pone.0096955.

[41] H. Chen, L. Chen, D. Liu, et al., Combined Clinical Phenotype and Lipidomic Analysis Reveals the Impact of Chronic Kidney Disease on Lipid Metabolism, J. Proteome Res. 16 (2017) 1566-1578. https://doi.org/10.1021/acs.jproteome.6b00956.

[42] B. Lidgard, A. N. Hoofnagle, L. R. Zelnick, et al., High-Density Lipoprotein Lipidomics and Mortality in CKD, Kidney Med. 5 (2023) 100708. https://doi.org/10.1016/j.xkme.2023.100708.

[43] Y. Chen, F. Torta, H. W. L. Koh, et al., Metabolomics profiling in multi-ancestral individuals with type 2 diabetes in Singapore identified metabolites associated with renal function decline, Diabetologia 68 (2025) 557-575. https://doi.org/10.1007/s00125-024-06324-z.

[44] F. Afshinnia, V. Nair, J. Lin, et al., Increased lipogenesis and impaired β-oxidation predict type 2 diabetic kidney disease progression in American Indians, JCI Insight 4 (2019) e130317. https://doi.org/10.1172/jci.insight.130317.

[45] K. Petkevicius, H. Palmgren, M. S. Glover, et al., TLCD1 and TLCD2 regulate cellular phosphatidylethanolamine composition and promote the progression of non-alcoholic steatohepatitis, Nat. Commun. 13 (2022) 6020. https://doi.org/10.1038/s41467-022-33735-6.

[46] F. Duranton, J. Laget, N. Gayrard, et al., The CKD plasma lipidome varies with disease severity and outcome, J. Clin. Lipidol. 13 (2019) 176-185.e8. https://doi.org/10.1016/j.jacl.2018.07.010.

[47] E. P. Rhee, C. B. Clish, A. Ghorbani, et al., A combined epidemiologic and metabolomic approach improves CKD prediction, J. Am. Soc. Nephrol. 24 (2013) 1330-1338. https://doi.org/10.1681/ASN.2012101006.

[48] Y. Hao, Y. Fan, J. Feng, et al., ALCAT1-mediated abnormal cardiolipin remodelling promotes mitochondrial injury in podocytes in diabetic kidney disease, Cell Commun. Signal. 22 (2024) 26. https://doi.org/10.1186/s12964-023-01399-4.

[49] Y. Wang, X. M. Zhou, X. Ma, et al., Construction of Nanodroplet/Adiposome and Artificial Lipid Droplets, ACS Nano 10 (2016) 3312-3322. https://doi.org/10.1021/acsnano.5b06852.

[50] M. V. Miles, The uptake and distribution of coenzyme Q10, Mitochondrion 7 Suppl(2007) S72-77. https://doi.org/10.1016/j.mito.2007.02.012.

[51] E. M. Mejia, H. Nguyen, and G. M. Hatch, Mammalian cardiolipin biosynthesis, Chem. Phys. Lipids 179 (2014) 11-16. https://doi.org/ 10.1016/j.chemphyslip.2013.10.001.

[52] Q. Yuan, B. Tang, and C. Zhang, Signaling pathways of chronic kidney diseases, implications for therapeutics, Signal Transduct. Target. Ther. 7 (2022) 182. https://doi.org/10.1038/s41392-022-01036-5.

[53] M. Guo, J. Gao, L. Jiang, et al., Astragalus Polysaccharide Ameliorates Renal Inflammatory Responses in a Diabetic Nephropathy by Suppressing the TLR4/NF-kappaB Pathway, Drug Des. Devel. Ther. 17 (2023) 2107-2118. https://doi.org/10.2147/DDDT.S411211.

[54] A. Ahmadi, A. P. Valencia, G. Begue, et al., Randomized Crossover Clinical Trial of Nicotinamide Riboside and Coenzyme Q10 on Metabolic Health and Mitochondrial Bioenergetics in CKD, medRxiv [Preprint] (2024). https://doi.org/10.1101/2024.08.23.24312501

[55] T. Gholnari, E. Aghadavod, A. Soleimani, et al., The Effects of Coenzyme Q10 Supplementation on Glucose Metabolism, Lipid Profiles, Inflammation, and Oxidative Stress in Patients With Diabetic Nephropathy: A Randomized, Double-Blind, Placebo-Controlled Trial, J. Am. Coll. Nutr. 37 (2018) 188-193. https://doi.org/10.1080/07315724.2017.1386140.

[56] A. Heidari, G. Hamidi, A. Soleimani, et al., Effects of Coenzyme Q10 Supplementation on Gene Expressions Related to Insulin, Lipid, and Inflammation Pathways in Patients With Diabetic Nephropathy, Iran. J. Kidney Dis. 12 (2018) 14-21.

[57] H. N. Bhagavan and R. K. Chopra, Coenzyme Q10: absorption, tissue uptake, metabolism and pharmacokinetics, Free Radic. Res. 40 (2006) 445-453. https://doi.org/10.1080/10715760600617843.

[58] A. Ochiai, S. Itagaki, T. Kurokawa, et al., Improvement in intestinal coenzyme q10 absorption by food intake, Yakugaku Zasshi 127 (2007) 1251-1254. https://doi.org/10.1248/yakushi.127.1251.

[59] P. H. Langsjoen and A. M. Langsjoen, Comparison study of plasma coenzyme Q10 levels in healthy subjects supplemented with ubiquinol versus ubiquinone, Clin. Pharmacol. Drug Dev. 3 (2014) 13-17. https://doi.org/10.1002/cpdd.73.